Unified prebiotically plausible synthesis of pyrimidine and purine RNA building blocks

Sidney Becker[1]*, Jonas Feldmann[1]*, Stefan Wiedemann[1]*, Hidenori Okamura[1], Christina Schneider[1], Katharina Iwan[1], Antony Crisp[1], Martin Rossa[1], Tynchtyk Amatov,[1] and Thomas Carell[1#]

[1]Center for Integrated Protein Science (CiPS[M]) at the Department of Chemistry, LMU München
Butenandtstr. 5-13, 81377 München
Fax: (+) 49 2180 77756
E-mail: Thomas.Carell@lmu.de
Homepage: www.carellgroup.de

Current affiliations:

Sidney Becker: Department of Chemistry, University of Cambridge, Lensfield Road, Cambridge, United Kingdom, CB2 1EW

Hidenori Okamura: Institute for Multidisciplinary Research for Advanced Materials, Tohoku University, 2-1-1 Katahira, Aoba-ku, Sendai, Miyagi 980-8577, Japan

Katharina Iwan: Centre for Translational Omics, University College London, Great Ormond Street Institute of Child Health, 30 Guilford Street, London, United Kingdom, WC1N 1EH

Tynchtyk Amatov: Max-Planck-Institut für Kohlenforschung, Kaiser-Wilhelm-Platz 1, 45470 Mülheim an der Ruhr, Germany

* These authors contributed equally

corresponding author: thomas.carell@lmu.de

One Sentence summary

Unified synthesis of pyrimidine and purine RNA building blocks under plausible prebiotic conditions.

Abstract

Theories about the origin of life require chemical pathways that allow formation of life's key building blocks under prebiotically plausible conditions. Complex molecules like RNA must have originated from small molecules whose reactivity was guided by physico-chemical processes. RNA is constructed from purine and pyrimidine nucleosides, both of which are required for accurate information transfer. This is the prerequisite for Darwinian evolution. While separate pathways to purines and pyrimidines have been reported, their concurrent syntheses remain a challenge. We report the synthesis of the pyrimidine nucleosides from small molecules and ribose, driven solely by wet-dry cycles. In the presence of phosphate-containing minerals, 5'-mono- and di-phosphates also form selectively in one-pot. The pathway is compatible with purine synthesis, allowing the concurrent formation of all Watson-Crick bases.

Introduction

The discovery of catalytic RNA[1] and the development of replicating RNA systems[2, 3] have lent strong support to the concept of an RNA world[4]. The RNA world hypothesis predicts that life started with RNAs that were able to (self)-recognize and replicate. Through a process of chemical evolution, a complex RNA and later RNA-peptide/protein world supposedly evolved, from which life ultimately emerged[4]. A prerequisite for the RNA world is the ability to create RNA under prebiotic conditions. This requires as the first elementary step the concurrent formation of pyrimidine and purine nucleosides in the same environment. Here, they must have condensed to form information carrying polymers able to undergo Darwinian evolution. The question of how the pyrimidine and purine nucleosides could have formed together is an unsolved chemical problem, under intensive chemical investigation[5-9]. Starting from an early atmosphere mainly composed of N_2 and CO_2,[10] the abiotic synthesis of life's building blocks must have occurred on the early Earth in aqueous environments, whose characteristics were determined by the minerals and chemical elements from which the early Earth's crust was made.[11, 12] Atmospheric chemistry, impact events and vulcanic activities must have provided the first reactive small molecules. These reacted in surface or deep-sea hydrothermal vents,[13-15] on mineral surfaces[16] or in shallow ponds.[17] Within these environments, volcanic activity, seasonal- or day-night cycles caused fluctuations of pH and temperature. Such fluctuating conditions provided wet-dry conditions allowing precipitation or crystallization of chemicals.[18] Mixing of micro-environments may have opened up new reaction pathways that led to increasing chemical complexity.

Along these geophysical boundaries, two main reaction pathways have been proposed for the formation of purine and pyrimidine nucleosides. The synthesis of the purines is possible along a continuous pathway based on the reaction of formamidopyrimidine (FaPy) precursors with ribose.[6, 18] For the pyrimidines a more stepwise reaction sequence involving aminooxazoles has been discovered.[5] These pathways provide the corresponding nucleosides under very different and partially incompatible conditions, leaving the question of how purines and pyrimidines could have formed in the same environment unanswered. Here, we report a prebiotically plausible pathway to pyrimidine nucleosides, which selectively provides the 5'-mono- and 5'-di-phosphorylated nucleosides as needed for RNA strand formation. By connecting the pathway with the reported purine route,[6, 18] we establish a unifying reaction network that allows for the simultanueous formation of both types of nucleosides in the same environment, driven by wet-dry cycles.

Results

Abiotic synthesis of pyrimidine nucleosides

The chemistry leading to pyrimidines starts from cyanoacetylene **1** as the key building block (Fig. 1A). Compound **1** is observed in interstellar clouds and in the atmosphere of Titan.(*19*) It has been shown to form in large quantities by electric discharge through an CH_4 / N_2 atmosphere(*20*) and is also a product of the Cu(II)-mediated reaction of HCN and acetylene in water (Fig. 1B2).(*21*) A recent report suggests that molecules such as **1** are plausible prebiotic starting materials, which could have formed in surface hydrothermal vents in significant concentrations.(*13*) We found that **1** reacts fast and cleanly with hydroxylamine **2** or hydroxylurea **3** to give 3-aminoisoxazole **4**. The reaction of **1** with **3** proceeds under slightly basic conditions (pH ~ 10) in $80 - 90\%$ yield within 2 h. **3** is formed in almost quantitative yields from the reaction of **2** with cyanate.(*22*) Compound **4** formed robustly even if we varied the temperature (10 - 95 °C), the reactant concentrations (10 - 100 mM) or added additional compounds such as urea **5** and/or different metal ions (see below). Reaction of cyanoacetylene **1** with hydroxylamine **2** gives **4** with 17% yield after 2 h at pH 10.

While hydroxylamine **2** is an accepted building block for prebiotic amino acid syntheses,(*23*) its potential formation on the early Earth is unclear. We therefore aimed to demonstrate its prebiotic availability. **2** is ultimately produced by reduction from NO, which is formed in large quantities when lightning passes through moist atmospheres containing N_2 and CO_2 (Fig. 1B).(*10*) NO forms as the main product under these conditions and spontaneously reacts in the presence of water to nitrite (NO_2^-) and nitrate (NO_3^-), which leads to the assumption that both anions were quite abundant on the early Earth.(*24-26*). With Fe(II) as a plausible prebiotic reductant, NO_2^- is converted to NH_3 but not to NH_2OH **2**.(*26*) Formation of the latter requires a partial reduction. We now found that this can be achieved with HSO_3^-, which forms from volcanic SO_2 and water.(*27*) NO_2^- and HSO_3^- react to **2** with up to 85% yield (Fig 1B, Fig. S1).(*28*) We confirmed, that this reaction gives first the hydroxylamine disulfonate **6** (Fig. 1B), which hydrolyses to hydroxylamine **2** and HSO_4^-. We find that intermediate **6** reacts with cyanoacetylene **1** as well (88% yield, Fig. 1B, FigS2) to give the stable olefin **7**, which upon hydrolysis provides again the key intermediate **4**. The overall yield of **4** via compound **7** is 63% over these two steps. The suggested pyrimidine intermediate **4** is therefore readily available from cyanoacetylene **1** upon reaction with either **2**, **3** or **6** under prebiotic conditions (Fig 1B).

When we added urea **5** to a solution of **4**, warming (70°C - 95°C) and dry-down resulted in formation of *N*-isoxazolyl-urea **8** (Fig. 1A and 2A) in a spot-to-spot reaction that is catalysed by Zn^{2+} or Co^{2+}. These metal ions were likely present on the early Earth.(*11, 12*) In the presence of Zn^{2+}, compound **8** is formed in 88% yield after 2 d at 95 °C (at 70 °C the same yield is obtained after ~2-3 w). With Co^{2+}, 68% yield is achieved after 2 d at 95 °C. The reaction of **4** to **8** is in all cases a clean process, with the only impurity being unreacted **4** (Fig. 2A). The product **8** can be subsequently physically enriched. Addition of carbonated water to the dried down reaction mixture solubilizes **4**, **5** and **8**, leaving the metal ions as hydroxides or carbonates behind. Subsequent concentration of the supernatant leads to spontaneous crystallization of **8** (55%). This allowed us to obtain a crystal structure of **8** (Fig. S3). In order to simulate early Earth chemistry, we performed a one-pot experiment. We mixed **1** with **3**, **5**, and Zn^{2+} or Co^{2+} in a carbonate solution (pH ~10) and indeed obtained compound **4** at 95°C (80-90%). Neutralizing the solution to pH ~6-7, which may have occurred on the early Earth due to acidic rain, followed by dry-down at the same temperature provided compound **8** with yields between 56% (Zn^{2+}) and 40% (Co^{2+}). The continuous synthesis of the key building block **8** was consequently achieved in a plausible prebiotic setting that could have existed in hydrothermal vents or near volcanic activity, both of which are able to provide elevated temperatures (Fig. S3). The synthesis is also possible at lower temperatures, but with extended reaction times.

For the final step towards nucleosides, we need to assume that, due to flooding or a mixing of environments, **8** came into contact with ribose **9** (Fig. 1A and 2B) or any other sugar unit such as threose (for TNA) or glyceraldehyde (for GNA) able to form a backbone for a pairing system.(*29, 30*) When we mixed **8** with ribose **9** and warmed up the mixture to 95 °C in the presence of boric acid, we observed a fast and

high-yielding reaction to provide the ribosylated products **10a-d** in 95% yield (Fig. S4a). Other borate minerals such as synthetic lüneburgite ($Mg_3[(PO_4)_2|B_2(OH)_6]\cdot 6H_2O$)(*31*) or borax ($Na_2[B_4O_5(OH)_4]\cdot 10H_2O$) were also able to catalyze this reaction,(*32*) giving high-yields (>70%, Fig. S5). The major products are initially the α/β-pyranosides (**10c** and **10d**), which dominate over the α/β-furanosides (**10a** and **10b**, Fig. S4a). After heating the mixture under slightly basic conditions at 95°C in the presence of borates, the furanosides (54%, **10a** and **10b,** Fig. 2A) gradually became the dominant products (Fig. S4b). Under these conditions we also observed hydrolysis of **10a-d** to **8** and **9**. The accumulation of the furanosides **10a** and **10b** is best explained by complexation of their *cis*-diols with borate.(*32*)

The final step towards pyrimidine nucleosides requires reductive opening of the isoxazole N-O bond, followed by tautomerisation, intramolecular cyclization and water elimination in a cascade-like fashion (Fig. 2C and 2D). We found that this reaction occurs rapidly with Fe^{2+} in the presence of thiols (Fig. 2D).(*33*) LC-MS analysis indicated that cytidine nucleosides **11a-d** formed efficiently under these conditions, with the furanosidic uridine nucleosides **12a,b** being the corresponding deamination products formed by hydrolysis (Fig. 2C). Reductive pyrimidine formation can be performed with FeS or the mineral pyrite (FeS_2), and both have been discussed in the context of early metabolic pathways.(*15, 34*) Just 0.0001 eq. of soluble Fe^{2+} in water is sufficient for the reaction. In the absence of Fe^{2+}, pyrimidine formation was not observed. The reduction also appears to be independent of the thiol source, as the products **11a-d** and **12a,b** are obtained regardless of whether we used dithiothreitol (DTT), propanedithiol, mercaptoethanol or cysteine (Fig. S6).

Selective one-pot formation of 5'-nucleoside mono- and di-phosphates

The addition of naturally occurring minerals such as hydroxyapatite, colemanite or (synthetic) lüneburgite to the reductive pyrimidine-forming reaction had a strong influence on the distribution of the four cytidine isomers. Synthetic lüneburgite gave a combined high yield of 85% (Fig. 2C). The natural furanosidic β-cytidine (**11b**) and its α-anomer (**11a**) are formed under these conditions with about the same yields together with small amounts of α- and β-uridine (**12a,b**). Importantly, we found only small amounts of the α- and β-cytidine pyranosides (**11c** and **11d**), together with the cytosine base. Since synthetic lüneburgite is known to enable nucleotide formation in the presence of urea (Fig. 3A),(*31*) we simply added urea to the one-pot reaction mixture after pyrimidine formation and allowed the mixture to evaporate to dryness at 85°C over a period of about 20 h. LC-MS analysis of the reaction now showed formation of phosphorylated nucleosides (Fig. 3A) in remarkable 19% yield relative to cytidine (Fig. 3B and Fig. S7). We assumed that the reaction generated the α- and β-cytidine-5'-mono-phosphates **13a/b** and the 5'-di-phosphorylated cytidines **14a/b**. Due to hydrolysis we also expected some α- and β-uridine-5'-mono- and 5'-di-phosphates **15a/b** and **16a/b**. We isolated the corresponding HPLC peaks and removed the phosphate groups enzymatically (Fig. 3B). LC-MS analysis showed now the dephosphorylated furanosides **11a/b** and **12a/b** with over 94% in the nucleoside pool, which corresponds to a change of the furanoside/pyranoside ratio from initially 4:1 to now 17:1 (Fig. 3B). The formation of phosphorylated pyranosides **17** are only a minor side reaction. We found no discrimination between α- and β-anomers during the phosphorylation. The furanoside enrichment is best explained by the presence of a primary hydroxyl group in the furanosides, which is absent in the pyranosides. The enrichment of 5'-nucleoside-(mono and di)-phosphates under these one-pot conditions consequently establishes a further chemical selection step that favors the furanosides as the components of RNA. We further characterized the structures of the phosphorylated nucleosides and confirmed the formation of the 5'-α- and 5'-β-cytidine-mono- and di-phosphates (**13/14a** and **b**, α-/β-CMP and α-/β-CDP, Fig. S8). Additional analysis allowed identification of α,β-UDP **16a/b** (Fig. S9). Interestingly, 5'-pyrophosphates are the dominating specie within the di-phophorylated nucleoside mixture (Fig S8a).

Compatible formation of pyrimidine and purine RNA nucleosides

We next investigated if the prebiotically plausible pyrimidine and purine nucleoside pathways are compatible with each other so that they can be connected with the goal to form all Watson-Crick building blocks in the same environment solely driven by wet-dry cycles. The purine synthesis(*18*) requires as the initial step reaction of malononitrile **18** with sodium nitrite to give (hydroxyimino)malononitrile **19**. Because malononitrile **18** can be also generated from cyanoacetylene **1**, as shown by Eschenmoser,(*35*) pyrimidines and purines can be traced back to the same chemical root (Fig. 4). Compound **19** forms an organic salt with amidines **20** to give nitroso-pyrimidines **21**, and upon reduction and formylation, formamidopyrimidines (FaPys, **22-25**). The latter can react with ribose **9** to give ribosylated FaPys **26** and then purine nucleosides **27**-**29** (Fig. 1A).(*18*) To investigate how the chemical conditions needed for pyrimidine formation from the urea-isoxazole **8** would affect purine formation, we reacted **8** and the FaPy-compounds **22** and **23** with ribose **9** under dry-down conditions. We performed the reaction under identical conditions but in separate reaction vials (Fig. 4). Under these conditions formation of all four Watson-Crick nucleosides cytidine **11,** uridine **12**, adenosine **27** and guanosine **28**, were detected.

We next investigated if pyrimidines and purines can form simultaneously in the same environment (Fig. 5A). For this experiment, we mixed the starting materials cyanoacetylene **1**, hydroxylurea **3**, (hydroxyimino) malononitrile **19** and amidine **20** under slightly basic conditions (pH ~10). Analysis of the mixture showed indeed formation of **4** in 86% yield, despite the presence of **19** and **20**. It is surprising that the N-OH functionality of compound **19** does not interfere with the formation of **4**. Compound **4** is a liquid that can enrich from a water solution by dry-down due to its high boiling point (228°C). Interestingly, **4** can act as a solvent to facilitate the formation of **21** from the reaction of **19** with **20** under milder conditions (50 °C – 100 °C instead of 126 °C) compared to a previous procedure.(*18*) The next step requires reduction and formylation of **21** to the FaPy intermediate, which, however, cannot be performed in the presence of the isoxazole. Addition of water, eventually containing urea **5**, led to spontaneous precipitation of **21**. The supernatant containing **4** and **5** can flow away. The water insoluble **21** if brought into contact with dilute formic acid and Zn (found in Earth's crust) reacts immediately to the compounds **22** and **24** and Zn^{2+} as a side product (Fig. 5A, Fig. S10a). The reaction products are now water soluble and can potentially recombine with **4** and **5**. The side product Zn^{2+} is now catalyzing the reaction of **4** in the presence of **5** to give the *N*-isoxazolyl-urea **8** in the presence of **22** and **24** (Fig. 5A, Fig S10b). This leads to the formation of the pyrimidine and purine precursors **8**, **22** and **24**, which can be transformed into the purine and pyrimidine nucleosides. In this scenario, the intermediate **4** of the pyrimidine pathway helps formation of the purine precursor **21** while Zn^{2+} as a side product of the purine pathway mediates formation of the pyrimidine precursor **8** in a mutually synergistic way, driven by wet-dry cycles.

We combined **8** with different FaPy-intermediates and investigated if they could react in a one-pot scenario with ribose **9** to finally give the purine and pyrimidine nucleosides. To examine this, we dissolved a mixture of **8**, **22**, **25**, ribose **9** and boric acid and warmed the mixture up to 95 °C for 14 h allowing for slow evaporation of water. The solid material was then taken up with a slightly basic solution containing Fe^{2+} (0.0005 eq.) and DTT (1.5 eq.), and we allowed the mixture to warm up to 95 °C. HPLC-MS analysis proved that these conditions simultaneously provided the purine and pyrimidine nucleosides with cytidine (**11a-d**) and adenosine (**27**) as the main products. Interestingly, diaminopurine nucleosides (DA, **29**), which hydrolyse to guanosine **28**, form in this one-pot reaction as well (Fig. 5A, chromatogram). We noted additional formation of double ribosylated adenine (rib$_2$-A). Furthermore, the nucleoside **28** can be created in this scenario if we use **23** (R^1 = OH, R^2 = NH_2) as the starting material but the yields were lower.

Discussion

Ribose based RNA and the four canonical nucleosides A, G, C and U are central to modern life and to prebiotic hypotheses such as the "RNA world", in which RNA strands replicated and evolved to give

increasingly complex chemical systems.(*4*) Whether such RNAs were directly assembled from the canonical nucleotides (A, C, G and U bases) or if it evolved from a simpler proto-RNA system is unclear.(*36*)

Here we show that a reaction network towards the purine and pyrimdine RNA building blocks can be established, starting from simple atmospheric or volcanic molecules. Molecular complexity is generated by wet-dry cycles that can drive the chemical transformations. Therefore any environment that was able to provide wet-dry phases might have been a suitable place for the origin of RNA building blocks. Our geochemical model assumes that chemistry took place within in several basins that were needed to locally separate intermediates. We also need one or two streams of water to allow exchange of soluble molecules (Fig. 5B). Intermediates might precipitate upon fluctuations of physico-chemical parameters allowing for the separation of soluble and insoluble materials (e.g. **4** and **21**). After further reactions, which re-establish solubility, the compounds can be recombined (Fig 5B). For our scenario we need to assume that the early Earth provided environmental conditions that fluctuated between slightly acidic (pH 3), potentially caused by acidic rain (SO_2, NO_x), or basic (pH = 10) caused by carbonates. Even though most of the chemistry described here is performed at elavated temperatures, the reactions also occur at lower temperatures, but with substantially longer reaction times. We can assume that temperatures fluctuated on the early earth just like today due to day-night or seasonal cycles. Such fluctuations would certainly have brought about wet-dry cycles, akin to our modern climate of drought and rain. All the geophysical requirements needed for the reported chemistry including elevated temperatures could have existed in geothermal fields or at surface hydrothermal vents, which are plausible geological environments on early Earth.

Our proposed chemical pathways towards pyrimidines and purines begin with cyanoacetylene **1**, which could have formed in surface hydrothermal vents.(*13*) Reaction of **2**, **3** and **6** with **1** is the starting point for the pyrimidines, but if **1** reacts instead with ammonia, a pathway to malononitrile **18** as the precursor for purine synthesis is possible (Fig. 4).(*35*) Another key molecule for the synthesis of purines and pyrimdines is NO_2^-, which is needed to nitrosate malonitrile **18** to **19**.(*18*) NO_2^- is also crucial for the formation of hydroxylamine in the presence of HSO_3^-, which is formed from volcanic SO_2.(*27*) The concentration of NO_2^- that is reachable in a prebiotic setting is under debate, but it is speculated that the most likely place for its accumulation are shallow ponds, as needed for our scenario.(*17*) In general, the limited stability of NO_2^- would not be an issue, provided that it is rapidly captured by HSO_3^- upon its formation. Our model assumes a surface environment, where molecules, such as NO_2^-, HSO_3^- or urea **5**, could have been delivered by rain after their formation in the atmosphere (Fig. 5B).(*25, 37*) Importantly, our chemistry shows that robust reaction networks can be established that allow all key intermediates to be generated efficiently from relatively complex mixtures, followed by their physical enrichment or separation on the basis of their solubility in water. Wet-dry cycles govern the formation of purine and pyrimidine RNA building blocks in a scenario depicted in Fig. 5B. Of course, we will be unable to definitively prove that the described scenario took indeed place on early Earth, but the reported chemistry shows that, under plausible prebiotic conditions, mutually synergistic reaction pathways can be established in which the intermediates along one pathway help the chemistry of the other. In such a scenario, we show that the key building blocks of life can be created without the need for sophisticated isolation and purification procedures of reaction intermediates, which is common in traditional organic chemistry.

Importantly, the concurrent formation of pyrimidine and purine nucleosides in the network can be traced back to just a handful of key starting molecules such as cyanoacetylene **1**, NH_3, NH_2OH **2** (or the disulfonate **6**), HCN, urea **5**, formic acid and isocyanate plus salts such as nitrites, carbonates and borates. Metals such as Zn or Fe and their ions play an important role in our chemistry, consistent with their proposed involvement in early metabolic cycles.(*23, 38*) In particular, iron-sulfur surfaces needed for pyrimidine formation are discussed as platforms for early prebiotic chemistry.(*15, 34, 39*) The 5'-(di)phosphorylation is integrated into our pathway if phosphate minerals such as lüneburgite or struvite (Fig. S11) are present. It remains unclear, however, how ribose or any other carbohydrate, such as glycerol or threose, needed to form the backbone of RNA or pre-RNA could have formed selectively.(*29, 40*) Sugars such as ribose can be

produced non-selectively in a formose-like reaction, which is possible in a variety of different physico-chemical environments.(*32, 41-43*)

REFERENCES AND NOTES

1. J. A. Doudna, T. R. Cech, The chemical repertoire of natural ribozymes. *Nature* **418**, 222-228 (2002).
2. D. P. Horning, G. F. Joyce, Amplification of RNA by an RNA polymerase ribozyme. *Proc. Natl. Acad. Sci.* **113**, 9786-9791 (2016).
3. J. Attwater, A. Raguram, A. S. Morgunov, E. Gianni, P. Holliger, Ribozyme-catalysed RNA synthesis using triplet building blocks. *eLife* **7**, e35255 (2018).
4. W. Gilbert, Origin of life: The RNA world. *Nature* **319**, 618 (1986).
5. M. W. Powner, B. Gerland, J. D. Sutherland, Synthesis of activated pyrimidine ribonucleotides in prebiotically plausible conditions. *Nature* **459**, 239 (2009).
6. S. Becker *et al.*, A high-yielding, strictly regioselective prebiotic purine nucleoside formation pathway. *Science* **352**, 833-836 (2016).
7. H.-J. Kim, S. A. Benner, Prebiotic stereoselective synthesis of purine and noncanonical pyrimidine nucleotide from nucleobases and phosphorylated carbohydrates. *Proc. Natl. Acad. Sci.* **114**, 11315-11320 (2017).
8. S. Stairs *et al.*, Divergent prebiotic synthesis of pyrimidine and 8-oxo-purine ribonucleotides. *Nat. Commun.* **8**, 15270 (2017).
9. R. Saladino *et al.*, Meteorite-catalyzed syntheses of nucleosides and of other prebiotic compounds from formamide under proton irradiation. *Proc. Natl. Acad. Sci.* **112**, E2746-E2755 (2015).
10. J. Kasting, Earth's early atmosphere. *Science* **259**, 920-926 (1993).
11. R. M. Hazen, Paleomineralogy of the Hadean Eon: A preliminary species list. *Am. J. Sci.* **313**, 807-843 (2013).
12. E. D. Swanner *et al.*, Cobalt and marine redox evolution. *Earth. Planet. Sci. Lett.* **390**, 253-263 (2014).
13. P. B. Rimmer, O. Shorttle, Origin of Life's Building Blocks in Carbon- and Nitrogen-Rich Surface Hydrothermal Vents. *Life* **9**, 12 (2019).
14. W. Martin, J. Baross, D. Kelley, M. J. Russell, Hydrothermal vents and the origin of life. *Nat. Rev. Microbiol.* **6**, 805 (2008).
15. E. Camprubi, S. F. Jordan, R. Vasiliadou, N. Lane, Iron catalysis at the origin of life. *IUBMB Life* **69**, 373-381 (2017).
16. S. A. Benner, H.-J. Kim, E. Biondi, in *Prebiotic Chemistry and Chemical Evolution of Nucleic Acids,* C. Menor-Salván, Ed. (Springer International Publishing, Cham, 2018), pp. 31-83.
17. S. Ranjan, Z. R. Todd, P. B. Rimmer, D. D. Sasselov, A. R. Babbin, Nitrogen Oxide Concentrations in Natural Waters on Early Earth. *Geochem. Geophys. Geosyst.* **20**, 2021-2039 (2019).
18. S. Becker *et al.*, Wet-dry cycles enable the parallel origin of canonical and non-canonical nucleosides by continuous synthesis. *Nat. Commun.* **9**, 163 (2018).
19. P. Thaddeus, The prebiotic molecules observed in the interstellar gas. *Philos. Trans. Royal Soc. B* **361**, 1681-1687 (2006).
20. R. A. Sanchez, J. P. Ferris, L. E. Orgel, Cyanoacetylene in Prebiotic Synthesis. *Science* **154**, 784-785 (1966).
21. B. H. Patel, C. Percivalle, D. J. Ritson, C. D. Duffy, J. D. Sutherland, Common origins of RNA, protein and lipid precursors in a cyanosulfidic protometabolism. *Nat. Chem.* **7**, 301 (2015).
22. H. Kofod, On the Isomerism of Hydroxyurea. I. Kinetics of the Reaction between Hydroxylammonium Ion and Cyanate Ion. *Acta Chem. Scand.* **7**, 274-279 (1953).
23. K. B. Muchowska, S. J. Varma, J. Moran, Synthesis and breakdown of universal metabolic precursors promoted by iron. *Nature* **569**, 104-107 (2019).
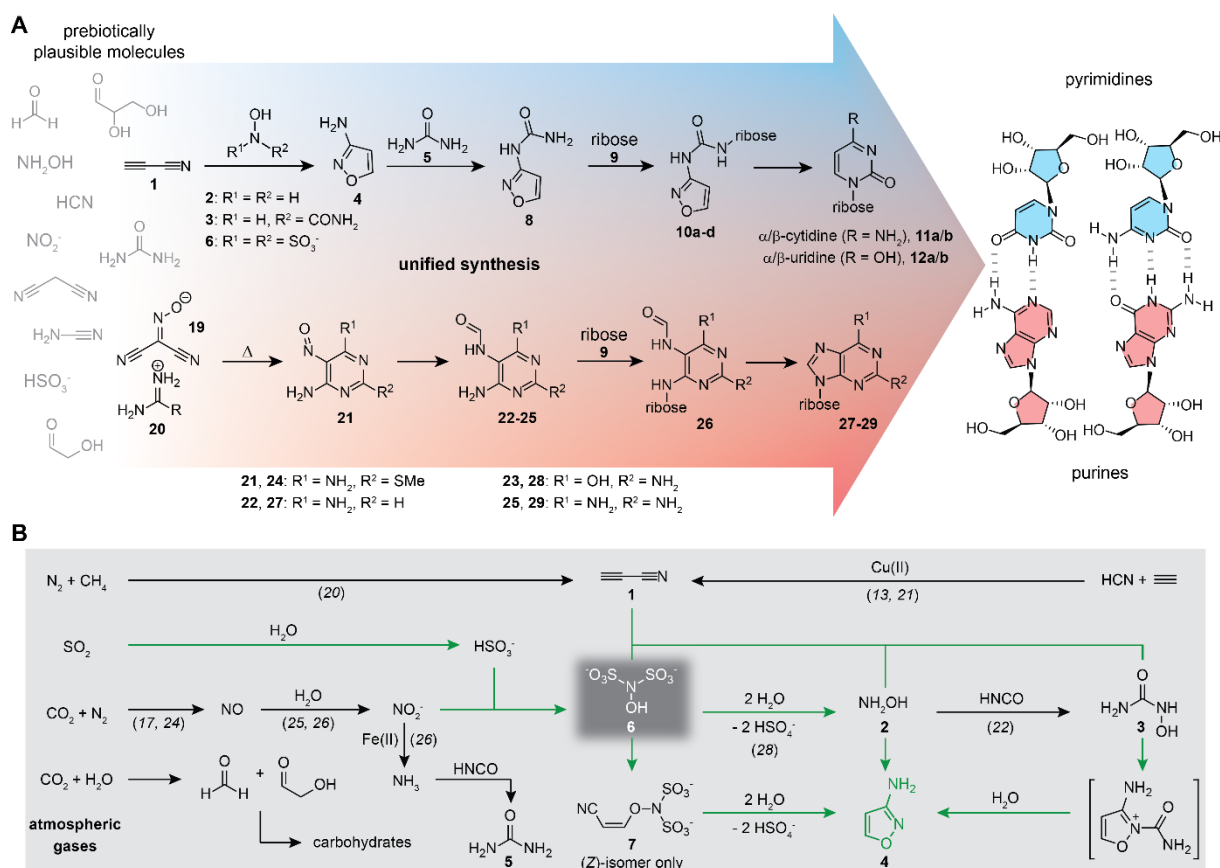
24. V. S. Airapetian, A. Glocer, G. Gronoff, E. Hébrard, W. Danchi, Prebiotic chemistry and atmospheric warming of early Earth by an active young Sun. *Nat. Geosci.* **9**, 452 (2016).

25. H. J. Cleaves, J. H. Chalmers, A. Lazcano, S. L. Miller, J. L. Bada, A Reassessment of Prebiotic Organic Synthesis in Neutral Planetary Atmospheres. *Orig. Life Evol. Biosphere* **38**, 105-115 (2008).

26. D. P. Summers, S. Chang, Prebiotic ammonia from reduction of nitrite by iron (II) on the early Earth. *Nature* **365**, 630-633 (1993).

27. R. Sukrit, T. Z. R., S. J. D., S. D. D., Sulfidic Anion Concentrations on Early Earth for Surficial Origins-of-Life Chemistry. *Astrobiology* **18**, 1023-1040 (2018).

28. G. K. Rollefson, C. F. Oldershaw, The reduction of nitrites to hydroxylamine by sulfites. *J. Am. Chem. Soc.* **54**, 977-979 (1932).

29. G. F. Joyce, The antiquity of RNA-based evolution. *Nature* **418**, 214 (2002).

30. D. M. Fialho *et al.*, Glycosylation of a model proto-RNA nucleobase with non-ribose sugars: implications for the prebiotic synthesis of nucleosides. *Org. Biomol. Chem.* **16**, 1263-1271 (2018).

31. K. Hyo-Joong *et al.*, Evaporite Borate-Containing Mineral Ensembles Make Phosphate Available and Regiospecifically Phosphorylate Ribonucleosides: Borate as a Multifaceted Problem Solver in Prebiotic Chemistry. *Angew. Chem. Int. Ed.* **55**, 15816-15820 (2016).

32. A. Ricardo, M. A. Carrigan, A. N. Olcott, S. A. Benner, Borate Minerals Stabilize Ribose. *Science* **303**, 196-196 (2004).

33. M. Kijima, Y. Nambu, T. Endo, Reduction of cyclic compounds having nitrogen-oxygen linkage by dihydrolipoamide-iron(II). *J. Org. Chem.* **50**, 1140-1142 (1985).

34. G. Wächtershäuser, Before enzymes and templates: theory of surface metabolism. *Microbiol. Rev.* **52**, 452-484 (1988).

35. U. Trinks, dir. A. Eschenmoser, ETH Zurich, Zurich (1987) (ETH e-collection 10.3929/ethz-a-000413538).

36. R. Krishnamurthy, On the Emergence of RNA. *Isr. J. Chem.* **55**, 837-850 (2015).

37. J. Liebig, F. Wöhler, Untersuchungen über die Cyansäure. *Ann. Phys.* **96**, 369-400 (1830).

38. M. Preiner *et al.*, A hydrogen dependent geochemical analogue of primordial carbon and energy metabolism. *bioRxiv*, 682955 (2019).

39. C. Bonfio *et al.*, Prebiotic iron–sulfur peptide catalysts generate a pH gradient across model membranes of late protocells. *Nat. Catal.* **1**, 616-623 (2018).

40. O. Trapp, J. Teichert, F. Kruse, Direct Prebiotic Pathway to DNA Nucleosides. *Angew. Chem. Int. Ed.* **0**.

41. J. Kofoed, J.-L. Reymond, T. Darbre, Prebiotic carbohydrate synthesis: zinc–proline catalyzes direct aqueous aldol reactions of α-hydroxy aldehydes and ketones. *Org. Biomol. Chem.* **3**, 1850-1855 (2005).

42. C. Meinert *et al.*, Ribose and related sugars from ultraviolet irradiation of interstellar ice analogs. *Science* **352**, 208-212 (2016).

43. K. Usami, A. Okamoto, Hydroxyapatite: catalyst for a one-pot pentose formation. *Org. Biomol. Chem.* **15**, 8888-8893 (2017).

ACKNOWLEDGEMENTS

the synthesis and MS quantification, K.I. performed biochemical studies, T.A. helped to design the synthesis. T.C., S.B., J.F., S.W. analysed data. T.C. and S.B. wrote the manuscript and designed the figures. **Competing interest:** The authors declare no competing interest. **Data and material availability:** The X-ray crystallographic data for isoxazoleurea **8** are deposited in the CCDC under accession number 1889652. All other data needed to support the conclusions of this manuscript are included in the main text and supporting material.

Figures

Fig. 1. Unified synthesis of pyrimidine and purine RNA building blocks. (**A**) Starting from plausible prebiotic molecules the reaction scheme depicts the route towards the pyrimdines *via* isoxazolylurea **8** (blue background) and the purines *via* formamidopyrimdines **22-25** (red background).(*18*) (**B**) Fundamental chemistry that produces the molecules needed for the pyrimidine pathway. Reactions performed in this work are shown with green arrows, while black arrows represent well known literature reactions. Formation of **4** requires reaction of **1** with hydroxylamine **2**, hydroxylurea **3** or the disulfonate **6** (dark grey box). **6** is formed from NO_2^- and SO_2/HSO_3^-.

Fig. 2. Formation of pyrimidine nucleosides (**11** and **12**) from *N*-isoxazolylurea-ribosides **10a/b**. The different isomers are labelled according to: **a** = α-furanosyl, **b** = β-furanosyl, **c** = α-pyranosyl, and **d** = β-pyranosyl. (**A**) Formation of **4** and its conversion with urea **5** to *N*-isoxazolylurea **8**. (**B**) Ribosylation of **8** with ribose **9** and equilibration of the reaction mixture in the presence of borates gives the furanosidic isomers **10a** and **10b** (54%). (**C**) Pyrimidine nucleoside formation by reductive N-O cleavage from the compound mixture **10a/b** in the presence of ammonium iron(II) sulfate hexahydrate (0.0005 eq.). The HPL-chromatogram with detection at 260 nm shows formation of cytidine (C, **11a-d**) and uridine (U, **12a/b**). (**D**) Proposed catalytic cycle for the Fe²⁺ catalysed reduction of the N-O bond of the isoxazole moiety.
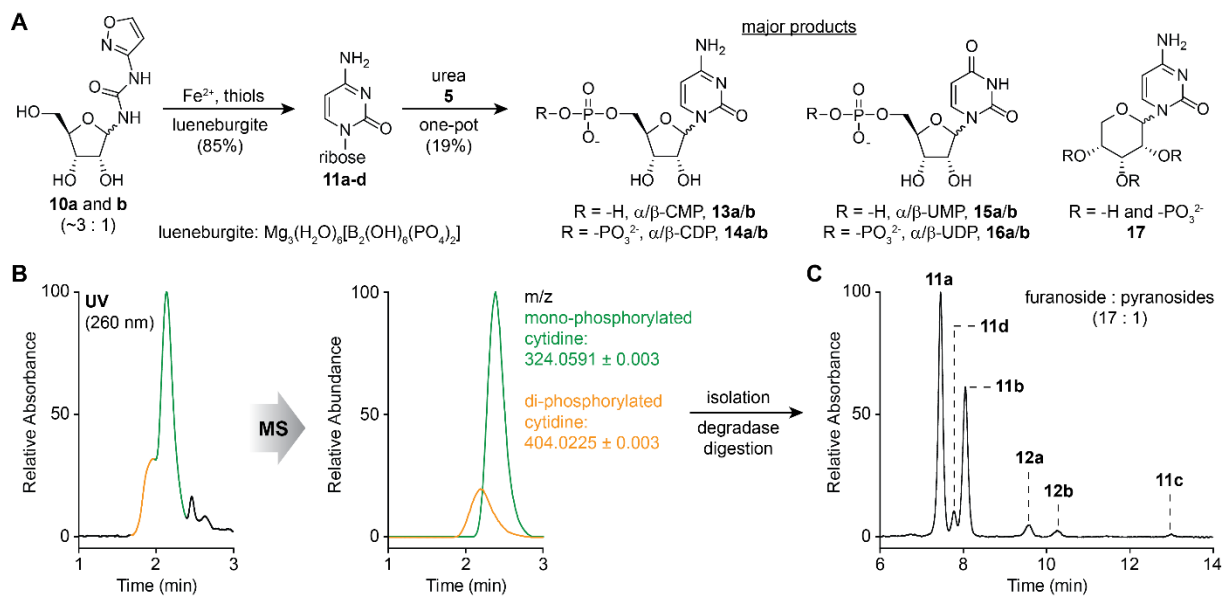
Fig. 3. One-pot nucleotide formation reaction. (**A**) One-pot synthesis of cytidine and uridine 5'-mono- and 5'-di-phosphates (**13a/b**-**16a/b**) after urea addition to the reaction mixture and allowing the mixture to dry-down at 85°C for 20 h. **a/b** represents the α- and β- anomers, respectively. (**B**) LC-MS analysis of the corresponding nucleotide peaks with UV- and MS-detection and isolation of the formed nucleotides from the prebiotic reaction, followed by an enzymatic removal of the phosphate groups. (**C**) HPLC analysis of the dephosphorylated product mixture showing predominant formation of α- and β-cytidine **11a** and **11b**.

11
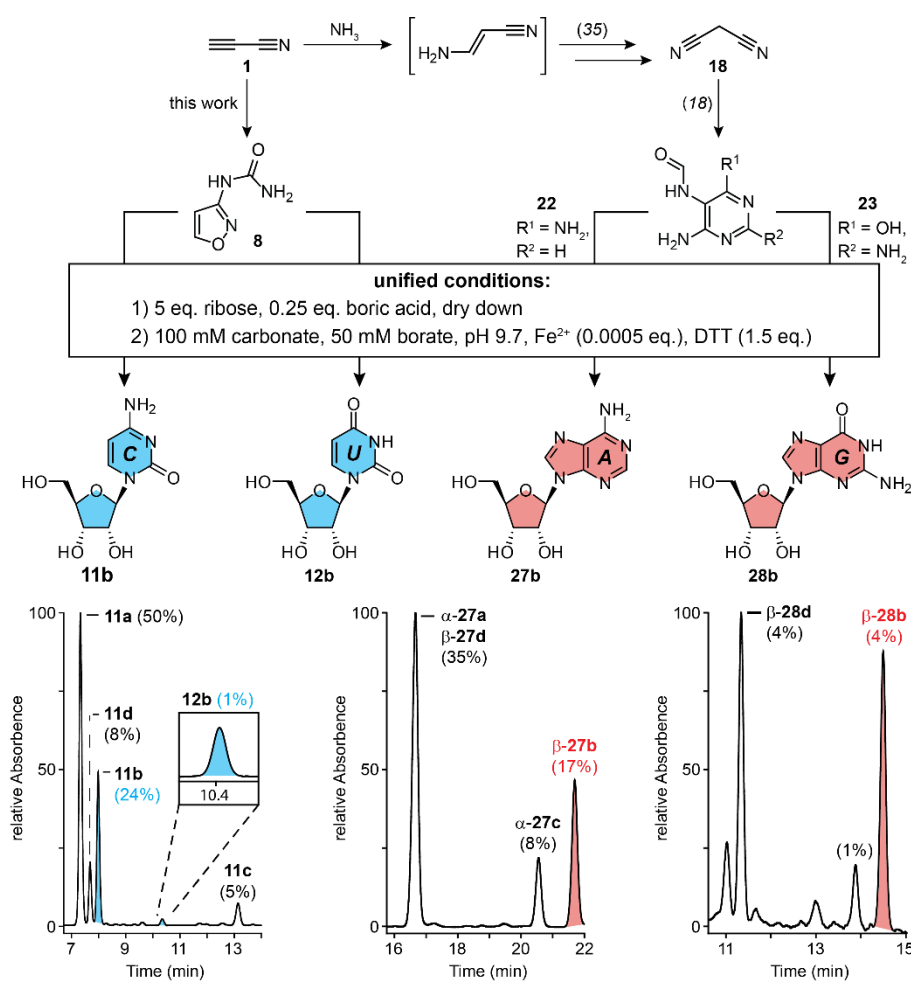
Fig. 4. Formation of all four Watson-Crick RNA building blocks in identical but parallel reactions. C (**11b**), U (**12b**), A (**27b**), and G (**28b**) are formed under the same conditions separately from **8**, **22** and **23**. HPL-chromatograms are shown with a detection at 260 nm. The nucleosides are labelled according to: **a** = α-furanosyl, **b** = β-furanosyl, **c** = α-pyranosyl, and **d** = β-pyranosyl. Canonical pyrimidine and purine RNA building blocks are labeled in blue or red, respectively.
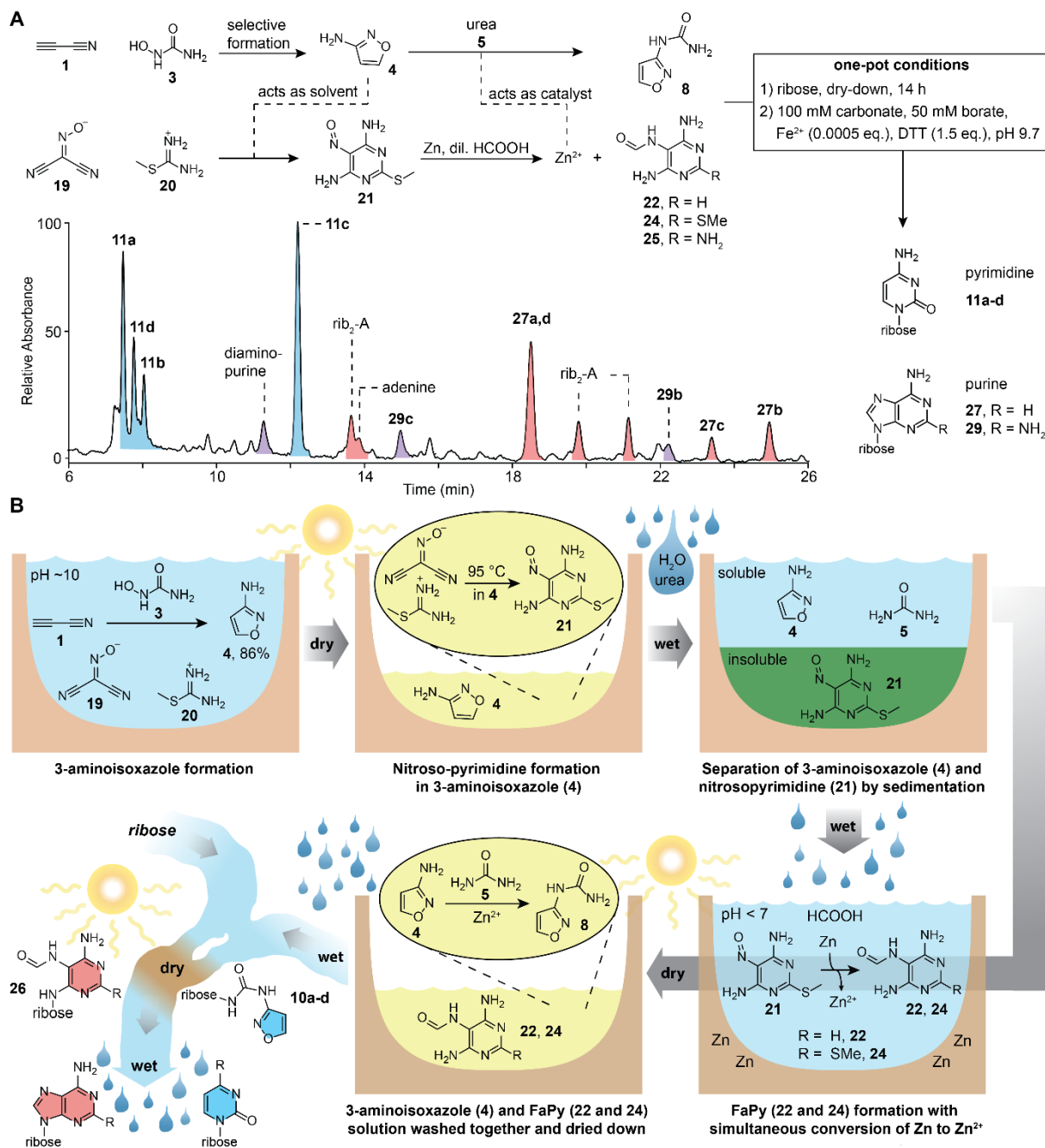
Fig. 5. Unified chemical scenario for the formation of purine and pyrimidine nucleosides. (**A**) Depiction of the connected reaction pathways to pyrimidine and purine nucleosides together with the HPLC analysis (260 nm) of the final reaction mixtures. (**B**) Proposed geochemical scenario for the simultaneous synthesis of purine and pyrimidine nucleosides, driven by wet-dry cycles. In yellow, the solvent is 3-aminoisoxazole (**4**), which can be enriched from an aqueous solution due to its high boiling point (228 °C). 2-(Methylthio)-5-nitrosopyrimidine-4,6-diamine (**21**) is a general precursor for adenosine and guanosine.(*18*) Compounds **8**, **22** and **24** are accessible in the same pot and they can react with ribose to the RNA nucleosides in a one-pot reaction. Nucleosides are labeled according to: **a** = α-furanosyl, **b** = β-furanosyl, **c** = α-pyranosyl, and **d** = β-pyranosyl.

13

Supplementary Materials for

Unified prebiotically plausible synthesis of pyrimidine and purine RNA building blocks

Sidney Becker*, Jonas Feldmann*, Stefan Wiedemann*, Hidenori Okamura, Christina Schneider, Katharina Iwan, Antony Crisp, Martin Rossa, Tynchtyk Amatov, and Thomas Carell[#]

*These authors contributed equally to this work.
[#]Corresponding author: thomas.carell@lmu.de

This PDF file includes:

Materials and Methods

<u>General Information</u>

Chemicals were purchased from Sigma-Aldrich, Fluka, ABCR, Carbosynth, TCI or Acros organics and used without further purification. The solvents were of reagent grade or purified by distillation. Chromatographic purification of products was accomplished using flash column chromatography on Merck Geduran Si 60 (40-63 μm) silica gel (normal phase). ^{1}H- and ^{13}C-NMR spectra were recorded on Varian Oxford 200, Bruker ARX 300, Varian VXR400S, Varian Inova 400, Bruker AMX 600 and Bruker AVIIIHD 400 spectrometers and calibrated to the residual solvent peak. Multiplicities are abbreviated as follows: s = singlet, d = doublet, t = triplet, q = quartet, m = multiplet, br = broad. High-resolution ESI spectra were obtained on the mass spectrometer Thermo Finnigan LTQ FT-ICR. IR measurements were performed on Perkin Elmer Spectrum BX FT-IR spectrometer with a diamond-ATR (Attenuated Total Reflection) setup. Melting points were measured on a Büchi B-540 device. For preparative HPLC purification a Waters 1525 binary HPLC Pump in combination with a Waters 2487 Dual Absorbance Detector was used, with a Nucleosil 100-7 C18 reversed phase column. The prebiotic reactions were analyzed by LC-ESI-MS on a Thermo Finnigan LTQ Orbitrap XL and were chromatographed by a Dionex Ultimate 3000 HPLC system. All chromatographic separations except for nucleotides were performed on an Interchim Uptisphere120 3HDO C18 column with a flow of 0.15 ml/min and a constant column temperature of 30 °C. Eluting buffers were buffer A (2 mM HCOONH$_4$ in H$_2$O (pH 5.5)) and buffer B (2 mM HCOONH$_4$ in H2O/MeCN 20/80 (pH 5.5)). The gradient for isoxazole containing compounds and pyrimidine nucleosides was 0 → 20 min, 0% → 4% buffer B. The gradient for purine nucleosides was 0 → 45 min, 0% → 15% buffer B. Chromatographic separation for nucleotides were performed on a YMC-Triart C18 column with a flow of 0.20 ml/min and a constant column temperature of 40 °C. Eluting buffers were buffer A (10 mM NH$_4$HCO$_3$ and 5 mM dibutylamine in H$_2$O (pH 9.1)) and buffer B (MeCN). The gradient was 0 → 10 min, 0% → 20%; 10 → 20 min, 20% → 20% buffer B. The elution was monitored at 223 nm and 260 nm (Dionex Ultimate 3000 Diode Array Detector). The chromatographic eluent was directly injected into the ion source without prior splitting. Ions were scanned by use of a positive polarity mode over a full-scan range of m/z 80-500 with a resolution of 30000. Nucleotides were scanned by use of a negative polarity mode over a full-scan range of m/z 120-1000 with a resolution of 30000. The synthetic standards for the co-injection experiments were synthesized in our lab (see synthetic procedures or according to reported literature(*44*)) or purchased. XRD measurements were performed on a STOE powder diffractometer in transmission geometry (Cu-Kα1, λ = 1.5406 Å) with a step size of 2°2θ (30 seconds per step) and equipped with a position-sensitive Mython-1K detector. The X-ray intensity data was measured at a temperature of 100 K on a Bruker D8 Venture TXS system equipped with a multilayer mirror optics monochromator and a Mo Kα rotating-anode X-ray tube (λ = 0.71073 Å). The frames were integrated with the Bruker SAINT software package using a narrow-frame algorithm. Data were corrected for absorption effects using the Multi-Scan method (SADABS). The structures were solved and refined using the Bruker SHELXTL software package.

Isolated nucleotides in 42 µL H_2O were digested as follows: 10X DNA Degradase™ Reaction Buffer (5 µL), together with 8 U DNA Degradase Plus™ (2 µL, Zymo Research) and 3.5 U of Benzonase® Nuclease (1 µL, Merck, purity >90%) was added and the mixture was incubated at 37 °C for 2 h. The sample was directly analysed by LC-MS according to the general information.

Apyrase digestion

Isolated nucleotides in 17.6 µL H_2O were digested as follows: 10X Apyrase reaction buffer (2 µL, NEB) was added together with 0.2 U of apyrase (0.4 µL, NEB). The mixture was incubated at 30 °C for 2 h. The sample was directly analysed by LC-MS according to the general information.

Synthetic Procedures
Hydroxylammonium chloride (2)

$HO-NH_3^+ \; Cl^-$

A solution of potassium hydroxylamine disulfonate **6** (269 mg, 1.00 mmol, 1.0 eq)(*45*) in 100 mM aq. HCl (10 mL) was shaken at 850 rpm and 90 °C for 2 h in an Eppendorf ThermoMixer®. The reaction mixture was treated with $BaCl_2$ (489 mg, 2.00 mmol, 2.0 eq) and left for 5 min at 90 °C to precipitate the formed sulfates. The resulting suspension was filtered, and the filtrate was lyophilized to afford a white residue, which was extracted with EtOH (3 x 5 mL). After removing the solvent *in vacuo*, hydroxylammonium chloride **2** was identified *via* ¹H-NMR (Fig. S1).

Note: Under neutral conditions, hydrolysis of hydroxylamine disulfonate proceeds over a much longer period of time.(*45, 46*)

¹H NMR (400 MHz, DMSO-*d₆*) δ 10.32 (s, 3H), 10.11 (s, 1H).

((2-Cyanovinyl)oxy)(sulfonato)sulfamate (7) *via* hydroxylamine disulfonate (6)
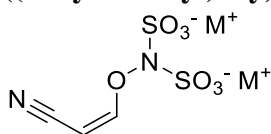
Prebiotically from SO_2 and NO_2^-:

$NaNO_2$ (2.76 g, 40.0 mmol, 1.0 eq) and $Na_2S_2O_5$ (4.18 g, 22.0 mmol, 0.55 eq) were dissolved in H_2O (150 mL). SO_2 was passed through the solution under stirring, while the temperature increased from 25 °C to about 35 °C. When a pH of 3 was reached, the gas injection was stopped and 700 µL of the reaction mixture were transferred into a microcentrifuge tube. After the successive addition of aq. Na_2CO_3 (300 µL, 1 M) and cyanoacetylene (6.26 µL, 100 µmol), the mixture was shaken at 25 °C and 850 rpm for 60 min in an Eppendorf ThermoMixer®. For quantification, a sample of 100 µL was treated with aq. 14.3 mM NaOAc (350 µL, as internal standard) and D_2O (50 µL). NMR spectroscopy (Fig. S2a) revealed the formation of (Z)-((2-cyanovinyl)oxy)(sulfonato)-sulfamate (7, 88%).

From hydroxylamine disulfonate:

To a solution of Na_2CO_3 (106 mg, 1.00 mmol, 2.2 eq.) and **6** (121 mg, 450 µmol, 1.0 eq) in H_2O (5 mL) was added cyanoacetylene (31.3 µL, 500 µmol, 1.1 eq.). The mixture was shaken at 25 °C and 850 rpm for 40 min in an Eppendorf ThermoMixer®. The mixture was neutralized with aq. 2 M HCl (500 µL) and lyophilized to obtain crude (Z)-((2-cyanovinyl)oxy)(sulfonato)sulfamate (**7**) as identified *via* NMR (Fig. S2b). Note: Compound **6** was synthesized according to literature.(*45*)

¹H NMR (400 MHz, D_2O) δ 7.38 (d, *J* = 7.0 Hz, 1H), 4.91 (d, *J* = 7.0 Hz, 1H). **¹³C NMR** (101 MHz, D_2O) δ 160.35, 115.47, 74.52. **HRMS** (ESI-): calc.: $[C_3H_3N_2O_7S_2]^-$ 242.9387, found: 242.9386 [M-H]⁻.

General procedure for the formation of 3-aminoisoxazole (4) under prebiotic conditions
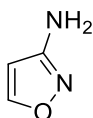
From hydroxyurea:

To a mixture of a divalent metal salt (13.6 mg $ZnCl_2$ or 23.8 mg $CoCl_2 \cdot 6\,H_2O$, 100 µmol, 1.0 eq.), Na_2CO_3 (42.4 mg, 400 µmol, 4.0 eq.), urea (24.0 mg, 400 µmol, 4.0 eq.), hydroxylurea (8.0 mg, 105 µmol, 1.1 eq.) in H_2O (1 mL) was added cyanoacetylene (6.26 µL, 100 µmol, 1.0 eq.). The mixture was shaken at 25 °C and 850 rpm for 2 h in an Eppendorf ThermoMixer®. A sample (10 µL) was taken and diluted with H_2O (990 µL) to 1 mL for LC-MS analysis (5 µL injection volume). Compound **4** was formed in 88% (Zn^{2+}) and 83% (Co^{2+}) yield, respectively. The yield was determined by LC-MS measurement with the calibration curve prepared using commercially available 3-aminoisoxazole. For the confirmation of the structural integrity, the reaction mixture was extracted with diethylether, dried over $MgSO_4$, concentrated and the crude residue purified by flash column chromatography (CH_2Cl_2:MeOH = 20:1). The NMR spectrum of the isolated compound was identical to that of a commercial sample.

From SO_2 and NO_2^-:

$NaNO_2$ (2.76 g, 40.0 mmol, 1.0 eq) and $Na_2S_2O_5$ (4.18 g, 22.0 mmol, 0.55 eq) were dissolved in H_2O (150 mL). SO_2 was passed through the solution under stirring, while the temperature increased from 25 °C to about 35 °C. When a pH of 3 was reached, the gas injection was stopped and 700 µL of the reaction mixture were transferred into a microcentrifuge tube. After the successive addition of aq. Na_2CO_3 (300 µL, 1 M) and cyanoacetylene (6.26 µL, 100 µmol), the mixture was shaken at 25 °C and 850 rpm for 60 min in an Eppendorf ThermoMixer®. To accelerate hydrolysis,(*46*) 900 µL of the reaction mixture were acidified with aq. conc. HCl (100 µL) and shaken at 50 °C and 850 rpm for 60 min in an Eppendorf ThermoMixer®. Compound **4** was formed in 63% yield. The yield was determined by LC-MS measurement with the calibration curve prepared using commercially available 3-aminoisoxazole.

From hydroxylamine:

To a mixture of $ZnCl_2$ (6.8 mg, 50 µmol, 0.5 eq), Na_2CO_3 (26.5 mg, 250 µmol, 2.5 eq), urea (12.0 mg, 200 µmol, 2.0 eq), 40% wt hydroxylamine (6.32 µL, 0.105 mmol, 1.1

eq) in H_2O (1 mL) was added cyanoacetylene (6.26 µL, 100 µmol, 1.0 eq). The mixture was shaken at 25 °C and 850 rpm for 3.5 h in an Eppendorf ThermoMixer®. A sample (10 µL) was taken and diluted with H_2O (990 µL) to 1 mL for LC-MS analysis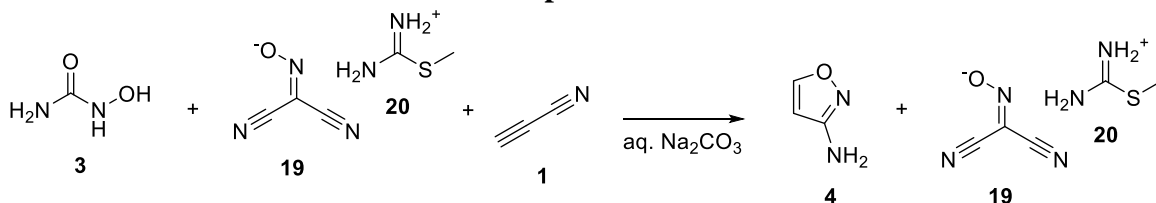 (5 µL injection volume). Compound **4** was formed in 17% yield. The yield was determined by LC-MS measurement with the calibration curve prepared using commercially available 3-aminoisoxazole.

¹H NMR (400 MHz, DMSO-d_6) δ 8.32 (d, J = 1.7 Hz, 1H, HC5), 5.88 (d, J = 1.7 Hz, 1H, HC4), 5.57 (s, 2H, NH_2). **¹³C NMR** (101 MHz, DMSO-d_6) δ 163.76 (C5), 158.73 (C3), 97.71 (C4).

N-isoxazolyl-urea (**8**)
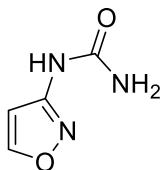
Prebiotic Synthesis from **4**:

To a solution of urea (120 mg, 2.00 mmol, 4.0 eq.) and a divalent metal salt (68 mg $ZnCl_2$ or 119 mg $CoCl_2$ · 6 H_2O; 0.5 mmol, 1.0 eq.) in H_2O (500 µL) was added 3-aminoisoxazole (36.9 µL, 500 µmol, 1.0 eq.). The mixture was shaken at 850 rpm and 95 °C for 2 d in an Eppendorf ThermoMixer® open to the air to allow water to evaporate. The resulting residue was dissolved in H_2O to a final volume of 1 mL. A sample (10 µL) was taken and diluted with H_2O (2000 x) for LC-MS analysis (5 µL injection volume). Compound **8** was formed in 88% (Zn^{2+}), 68% (Co^{2+}) and 25% (no metal) yield, respectively. The yield was determined by LC-MS measurement with the calibration curve prepared using synthetic *N*-isoxazolyl-urea.

For prebiotic enrichment, five replicates of the aforementioned reaction were prepared using $ZnCl_2$. The crude products were combined and resuspended in H_2O (50 mL). After treatment with K_2CO_3 (2.76 g, 20 mmol, 4.0 eq.) in H_2O (10 mL), the resulting suspension was mixed and centrifuged at 5000 rpm for 5 min. The supernatant was transferred into a 100 mL beaker and left at RT for 5 d to allow for crystallization by concentration. Crystallized *N*-Isoxazolyl-urea (348 mg, 2.74 mmol, 55%) was collected and analyzed by X-ray spectroscopy.

One-pot prebiotic synthesis from **1**:

To a mixture of a divalent metal salt (13.6 mg $ZnCl_2$ or 23.8 mg $CoCl_2$ · 6 H_2O; 100 µmol, 1.0 eq.), Na_2CO_3 (42.4 mg, 400 µmol, 4.0 eq.), urea (24.0 mg, 400 µmol, 4.0 eq.), hydroxylurea (8.0 mg, 105 µmol, 1.1 eq.) in H_2O (1 mL) was added cyanoacetylene (6.26 µL, 100 µmol, 1.0 eq.). The suspension was shaken at 25 °C and 850 rpm for 2 h in an Eppendorf ThermoMixer®. The mixture was neutralized with conc. aq. HCl (70.4 µL) and left to equilibrate for several minutes at 95 °C to adjust the pH to ~6-7. The resulting solution was shaken at 95 °C and 850 rpm for 2 d in an Eppendorf ThermoMixer® open to the air to allow water to evaporate. The resulting residue was dissolved in H_2O to a final volume of 1 mL. A sample (10 µL) was taken and diluted with H_2O (990 µl) to 1 mL for LC-MS analysis (5 µL injection volume). Compound **8** was formed in 56% (Zn^{2+})

and 40% (Co^{2+}) yield, respectively. The yield was determined by LC-MS measurement with the calibration curve prepared using synthetic N-isoxazolyl-urea.

Synthetic reference:

3-aminoisoxazole (1.14 g, 1.00 ml, 13.5 mmol) was dissolved in dry THF (20 ml) under inert atmosphere at 0°C. 2,2,2-trichloroacetylisocyanate (2.45 g, 1.61 ml, 13.5 mmol) was slowly added to the solution and the reaction was stirred at rt for 2 h. The reaction was quenched with MeOH (10 ml) and the solvent removed *in vacuo*. After co-evaporation with EtOH (2 x 20 ml) the product was obtained as a colorless solid (3.44 g, 12.6 mmol, 93 %). The crude product (3.12 g, 11.4 mmol) was dissolved in methanolic ammonia (10 mL, 7 M) and stirred for 1.5 h at rt. MeOH (20 mL) und EtOH (20 mL) were added to the reaction to obtain a clear solution. Et_2O (40ml) was added to the clear solution to precipitate the product. The crude product was filtered off and was subsequently dissolved in H_2O (20 ml). After filtering through celite, the solvent was removed by freeze-drying to obtain the product as a colorless solid (1.16 g, 9.15 mmol, 80%).

mp: 175 °C. **^{1}H NMR** (400 MHz, DMSO-d_6) δ (ppm) = 9.41 (s, 1H, HN4), 8.65 (d, ^3J = 1.7 Hz, 1H, HC5), 6.70 (d, ^3J = 1.7 Hz, 1H, HC4), 6.28 (s, 2H, NH_2).**^{13}C NMR** (101 MHz, DMSO-d_6) δ (ppm) = 159.4 (C5), 158.6 (C3), 154.6 (CO), 98.2 (C4). **HRMS** (ESI+): calc.: $[C_4H_6N_3O_2]^+$ 128.0455, found: 128.0455 $[M+H]^+$. **IR** (cm^{-1}): $\tilde{\nu}$ = 3486 (vw), 3389 (w), 3259 (vw), 3179 (w), 3194 (w), 3033 (w), 2958 (w), 1752 (m), 1730 (m), 1686 (w), 1631 (w), 1592 (vs), 1537 (w), 1486 (m), 1416 (s), 1378 (s), 1343 (w), 1298 (vw), 1284 (w), 1123 (m), 1070 (w), 1039 (vw), 981 (vw), 928 (w), 891 (w), 797 (s), 756 (vs), 654 (w).

Formation of 3-aminoisoxazole 4 in the presence of 19 and 20

To a solution of the methylthioamidine **20** salt of (hydroxyimino)malononitrile **19** (9.3 mg, 50 µmol, 0.5 eq), Na_2CO_3 (26.5 mg, 250 µmol, 2.5 eq.), and hydroxylurea **3** (8.0 mg, 0.11 µmol, 1.1 eq.) in H_2O (1 mL) was added cyanoacetylene (6.26 µL, 100 µmol, 1.0 eq). The mixture was left at rt for 10 min. A sample (10 µL) was taken and diluted with H_2O (990 µL) to 1 mL for LC-MS analysis (5 µL injection volume). Compound **4** was formed in 86% yield. The yield was determined by LC-MS measurement with the calibration curve prepared using commercially available 3-aminoisoxazole.

Prebiotically linked syntheses of pyrimidine (8) and purine (22,24) precursors (see Fig. 5 and Fig. S10)

R = SMe (**24**)
R = H (**22**)
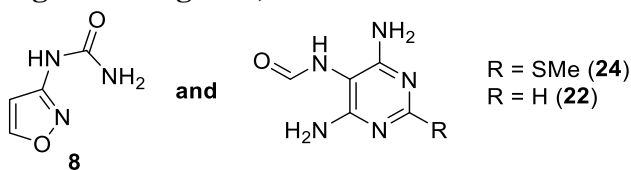
(A) Formation of 2-(methylthio)-5-nitrosopyrimidine-4,6-diamine **21**
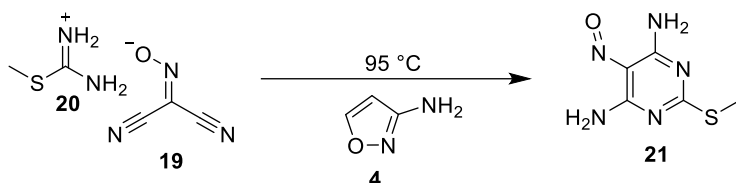
The methylthioamidine salt of (hydroxyimino)malononitrile (130 mg, 0.7 mmol, 0.5 eq.) was suspended in 3-amino-isoxazole (103 µL, 1.39 mmol, 1 eq.) and shaken at 95 °C and 850 rpm for 3 h in an Eppendorf ThermoMixer®. To the reaction mixture was added an aq. solution of urea (4 eq. in 1 mL H_2O). The reaction mixture was filtered, the residue was washed with H_2O (1 mL) and dried to afford crude 2-(methylthio)-5-nitroso-pyrimidine-4,6-diamine **21** (57 mg, 0.31 mmol, 45%). The filtrate was kept for the formation of **8**.

(B) Formation of formamidopyrimidine **22** and **24**
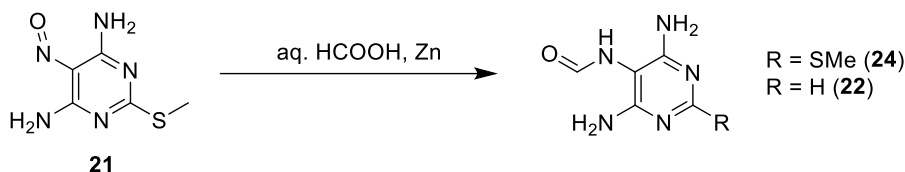
The intermediate **21** (46 mg, 0.25 mmol, 1.0 eq) was suspended in aq. HCOOH (4.5%, 2.5 mL) in the presence of elementary Zn powder (65 mg, 1.0 mmol, 4.0 eq). The reaction mixture was stirred at 70 °C in a sealed 15 mL Ace pressure tube for 4 h. After cooling to rt, the mixture was diluted with H_2O (2.5 mL) and filtered. The filtrate was analysed by LC-MS (see Fig. 5b) and was used for the formation of **8** in the next step.

(C) Formation of isoxazolyl-urea **8**
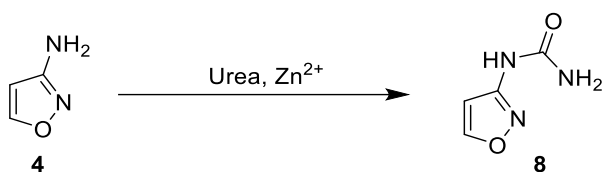
The filtrate from (B) was transferred into a conical glass tube containing the filtrate of (A). The solution was left at 95 °C for 2d in the oven open to the air to allow water to evaporate. After cooling to rt, the resulting solid was suspended in H_2O (10 mL). A sample (100 µL) was taken and diluted with H_2O (10 x) for LC-MS analysis (5 µL injection volume). FaPyA (**22**), FaPyms^{2}A (**24**) and *N*-isoxazolyl-urea (**8**), were observed as main products (see Fig. 5c).

N-isoxazolyl-N'-ribosyl-urea (10a-d)
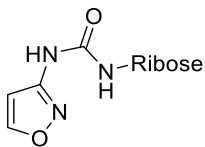
Prebiotic synthesis:

   N-isoxazolylurea (6.4 mg, 0.05 mmol) was thoroughly ground up with ribose (37.5 mg, 0.25 mmol, 5 eq.) and boric acid (0.8 mg, 0.013 mmol, 0.25 eq.). The mixture was heated overnight in an oven at 95 °C. Alternatively the reaction can also be performed by a dry-down method, where a solution of *N*-isoxazolylurea (500 ul, 0.05 mmol, 100 mM) is mixed with a ribose (83 µl, 0.25 mmol, 3 M) and boric acid (25 ul, 0.013 mmol, 500 mM) solution. The mixture was kept in an oven for 20 h at 95 °C. The sample was dissolved in H_2O (2 ml) and analyzed by LC-MS. To confirm the structural integrity, the different isomers were isolated by reversed phase HPLC in pure form.

Synthetic reference:

   1-*O*-acetyl-2,3,5-tri-*O*-benzoyl-β-D-ribofuranose (17.0 g, 33.8 mmol) was dissolved in dry DCM (300 ml) under inert atmosphere. $TiCl_4$ (4.46 mL, 40.7 mmol) was added and stirred for 2 h at rt. H_2O (250 ml) was added and filtered through celite. The organic layer was separated and the aqueous phase was extracted with DCM (3 x 100 ml). The combined organic layers were washed with sat. NaCl (300 ml), dried over $MgSO_4$, filtered and the solvent was removed *in vacuo*. The crude product was dissolved in dry toluene (300 ml) and AgNCO (6.25 g, 41.6 mmol) was added. After refluxing for 2.5 h, the reaction mixture was filtered through celite and washed with dry toluene. To the clear solution was added 3-aminoisoxazole (3 ml, 40.6 mmol) and stirred for 16 h at rt. The solvent was removed *in vacuo* and the product purified by flash column chromatography (DCM:MeOH 50:1). The product was dissolved in methanolic ammonia (330 ml, 7 M) and stirred for 18 h at rt. The solvent was removed *in vacuo* and the product purified by flash column chromatography (DCM:MeOH 17:3 → 4:1). The product was obtained as a colorless foam and contained a 3:1 mixture of the α- and β-furanoside (4.87 g, 18.8 mmol, 56%). The α- and β-furanosides were isolated in pure form by reversed phase HPLC to confirm the structural integrity.

α-furanosyl-isomer 10a
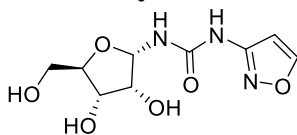
   mp: (131 °C).**¹H NMR** (400 MHz, DMSO-*d₆*) δ (ppm) = 9.85 (s, 1H, NH), 8.66 (d, ^3J = 1.7 Hz, 1H, HC5), 7.24 (d, ^3J = 9.5 Hz, 1H, C1'NH), 6.73 (d, ^3J = 1.8 Hz, 1H, HC4), 5.50 (dd, ^3J = 9.5, 4.4 Hz, 1H, HC1'), 5.41 (br, 1H, C3'OH), 5.03 (br, 1H, C2'OH), 4.66 (br, 1H, C5'OH), 3.92 (t, ^3J = 4.4 Hz, 1H, HC2'), 3.87 (dd, ^3J = 6.6, 4.5 Hz, 1H, HC3'), 3.71 (ddd, J = 6.5, 4.9, 3.1 Hz, 1H, HC4'), 3.49 (dd, ^2J = 11.7 Hz, ^3J = 3.1 Hz, 1H, H_aC5'), 3.39-3.35 (m, 1H, H_bC5'). **¹³C NMR** (101 MHz, DMSO-*d₆*) δ (ppm) = 159.5 (C5), 158.4 (C3), 153.3 (CO), 98.3 (C4), 81.9 (C4'), 80.6 (C1'), 71.1 (C3'), 70.1 (C2'), 61.6 (C5'). **HRMS** (ESI+): calc.: $[C_9H_{14}N_3O_6]^+$ 260.0877, found: 260.0877 $[M+H]^+$. **IR**

(cm^{-1}): $\tilde{\nu}$ = 3852 (w), 3820 (w), 3648 (w), 3283 (w)m 1843 (vw), 1771 (w), 1717 (m), 1699 (s), 1652 (vs), 1634 (s), 1575 (m), 1558 (vs), 1539 (vs), 1506 (vs), 1456 (s), 1436 (m), 1418 (m), 1032 (m), 971 (m).

β-furanosyl-isomer 10b
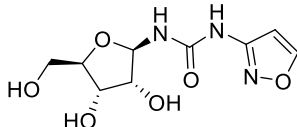
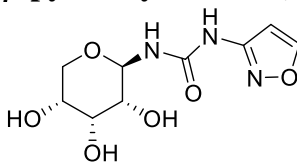**mp**: 120 °C (decomp.). **^{1}H NMR** (400 MHz, DMSO-d_6) δ (ppm) = 9.63 (s, 1H, NH), 8.67 (d, ^3J = 1.7 Hz, 1H, HC5), 7.13 (d, ^3J = 9.5 Hz, 1H, C1'NH), 6.74 (d, ^3J = 1.7 Hz, 1H, HC4), 5.20 (dd, ^3J = 9.5, 5.4 Hz, 1H, HC1'), 5.12 – 4.68 (m, 3H, C2'OH, C3'OH and C5'OH), 3.85 (t, ^3J = 4.6 Hz, 1H, HC3'), 3.71 (t, ^3J = 5.4 Hz, 1H, HC2'), 3.67 (q, ^3J = 4.2 Hz, 1H, HC4'), 3.45 (dd, ^2J = 11.7 Hz, ^3J = 4.0 Hz, 1H, H$_a$C5'), 3.42 – 3.39 (m, 1H, H$_b$C5'). **^{13}C NMR** (101 MHz, DMSO-d_6) δ (ppm) = 159.6 (C5), 158.3 (C3), 153.4 (CO), 98.3 (C4), 84.4 (C1'), 83.5 (C4'), 74.3 (C2'), 70.3 (C3'), 61.8 (C5'). **HRMS** (ESI+): calc.: [C$_9$H$_{13}$NaN$_3$O$_6$]$^+$ 282.0697, found: 282.0696 [M+Na]$^+$. **IR** (cm^{-1}): $\tilde{\nu}$ = 3268 (m), 1677 (m), 1599 (s), 1537 (vs), 1478 (s), 1403 (m), 1228 (m), 999 (vs), 893 (s), 777 (vs).

α-pyranosyl-isomer (10c)
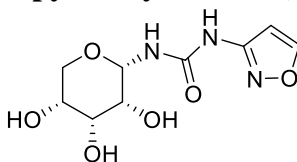
mp: 190 °C. **^{1}H NMR** (400 MHz, DMSO-d_6) δ (ppm) = 9.97 (s, 1H, NH), 8.67 (d, ^3J = 1.8 Hz, 1H, HC5), 7.47 (d, ^3J = 9.1 Hz, 1H, C1'NH), 6.74 (d, ^3J = 1.8 Hz, 1H, HC4), 5.25 – 4.87 (m, 4H, HC1', C2'OH, C3'OH, C5'OH), 3.70 (t, ^3J = 2.8 Hz, 1H, HC3'), 3.64 – 3.44 (m, 4H, HC2', HC4', H$_a$C5', H$_b$C5'). **^{13}C NMR** (101 MHz, DMSO-d_6) δ (ppm) = 159.5 (C5), 158.4 (C3), 153.4 (CO), 98.4 (C4), 77.9 (C1'), 69.4 (C3'), 69.3 (C4'), 68.4 (C5') 67.6 (C2'). **HRMS** (ESI+): calc.: [C$_9$H$_{13}$N$_3$O$_6$]$^+$ 260.0877, found: 260.0877 [M+H]$^+$. **IR** (cm^{-1}): $\tilde{\nu}$ = 3090 (vw), 2363 (m), 2271 (w), 1956 (w), 1700 (vs), 1683 (s), 1652 (s), 1823 (w), 1732 (w), 1700 (vs), 1683 (s), 1652 (s), 1609 (w), 1559 (m), 1509 (m), 1456 (s), 707 (w), 680 (m), 656 (s).

β-pyranosyl-isomer (10d)

mp: 175 °C (decomp.). **^{1}H NMR** (400 MHz, DMSO-d_6) δ (ppm) = 9.46 (s, 1H, NH), 8.68 (d, ^3J = 1.8 Hz, 1H, HC5), 6.89 (d, ^3J = 9.1 Hz, 1H, C1'NH), 6.74 (d, ^3J = 1.8 Hz, 1H, HC4), 4.90 (t, ^3J = 9.1 Hz, 1H, HC1'), 4.84 (d, ^3J = 3.6 Hz, 1H, C3'OH), 4.82 (d, J = 7.4 Hz, 1H, C2'OH), 4.69 (d, ^3J = 6.5 Hz, 1H, C4'OH), 3.88 (q, J = 2.8 Hz, 1H, HC3'), 3.55 – 3.47 (m, 1H, HC4'), 3.47 – 3.37 (m, 2H, H$_a$C5', H$_b$C5'), 3.18 (ddd, J =

9.1, 7.4, 2.8 Hz, 1H, HC2'). **^{13}C NMR** (101 MHz, DMSO-d_6) δ (ppm) = 159.7 (C5), 158.3 (C3), 153.6 (CO), 98.3 (C4), 77.5 (C1') 70.9 (C3'), 69.9 (C2'), 67.0 (C4'), 64.1 (C5'). **HRMS** (ESI+): calc.: $[C_9H_{13}N_3O_6]^+$ 260.0877, found: 260.0877 $[M+H]^+$. **IR** (cm^{-1}): $\tilde{\nu}$ = 3314 (m), 2871 (vw), 1941 (vw), 1705 (vs), 1598 (w), 1540 (vs), 1476 (w), 1432 (vw), 1336 (vw), 1282 (m), 1266 (w), 1208 (w), 1168 (m), 1139 (m), 1088 (w), 1065(m), 1035 (vs), 1004 (m), 950 (s), 916 (w), 886 (m), 804 (m), 789 (vs), 744 (w), 706 (m).

Prebiotic formation of pyrimidine nucleosides and nucleotides

General procedure nucleoside formation

The reactions were handled under inert atmosphere. All solutions were degassed for 1 h with argon before use. A solution of ribose isoxazole **10a/b** as a 3:1 mixture (25.9 mg, 0.1 mmol, 1 eq.) in 75 mM Na_2CO_3 (0.5 ml) was added to a mixture of mineral (1 eq.), dithiol (1.5 eq.) and Fe^{2+} source (0.5 eq.) in a 15 ml falcon tube. The tube was sealed with a PTFE sealing tape and shaked for 4 h at 100°C in an Eppendorf ThermoMixer®. After cooling to rt, it was centrifuged and a sample (10 µL) was removed and diluted with H_2O to 1 ml. This diluted sample was used for LC-MS analysis according to the general information.

The different minerals, thiols and iron sources used are stated in the main text. Monothiols were used with 3 eq. As water soluble Fe^{2+} salt we used ammonium iron(II) sulfate hexahydrate in a range of 0.001-0.0001 eq. Reactions without minerals were performed in a different buffer (100 mM Na_2CO_3, 50 mM boric acid, pH 9.7).

General procedure for one-pot nucleotide formation

The above described procedure was used for nucleoside formation. Lüneburgite or struvite (0.1 mmol, 1 eq.) were used as minerals, DTT (23.1 mg, 0.15 mmol, 1.5 eq.) and FeS_2 (6.0 mg, 0.05 mmol, 0.5 eq.) were used as thiol and Fe^{2+} source. After nucleoside formation we added solid urea (240 mg, 4 mmol, 40 eq.) and in case of struvite additionally oxalic acid (0.30 mmol, 3.0 eq.). The mixture was heated to 65 °C until the urea was fully dissolved. The sample was well suspended by vortexing and a sample (25 µL) was transferred into a 2 ml Eppendorf tube. The sample was kept at 85 °C for 20 h in an Eppendorf ThermoMixer® open to the air to allow water to evaporate. The dried sample was taken up in H_2O (1 ml) and analyzed for nucleotides by LC-MS analysis according to the general information.

Formation of purine nucleosides compatible to pyrimidine nucleoside formation

For purine nucleoside synthesis, FaPyA **22** or FaPyG **23** (0.05 mmol, 1eq.) was thoroughly ground up with ribose (37.5 mg, 0.25 mmol, 5 eq.) and boric acid (0.80 mg, 0.013 mmol, 0.25 eq.), identical to the N-isoxazolyl-urea ribosylation. The mixture was heated overnight in an oven at 95 °C. The resulting ribosides were heated at 100 °C in sealed 2 ml Eppendorf tubes under the following conditions: 100 mM Na_2CO_3, 50 mM boric acid, pH 9.7, 1.5 eq. DTT and 0.0005 eq. ammonium iron(II) sulfate hexahydrate. The following reaction times and concentrations were used: FaPyA (3d, 25 mM), FaPyG (2d, 6.25 mM).

Formation of purine and pyrimidine nucleoside in an one-pot reaction

For one-pot nucleoside synthesis of purines and pyrimidines, solutions of **8** (400 μl, 100 mM, 40 μmol, 1.0 eq), FaPyA (400 μl, 50 mM, 20 μmol, 0.5 eq.), FaPyDA (400 μL, 50 mM, 20 μmol, 0.5 eq.), ribose (267 μL, 3 M, 800 μmol, 20 eq.) and boric acid (48.0 uL, 500 mM, 24 μmol, 0.6 eq.) were heated at 95 °C for 14 h in a dry down reaction. The formed residue containing **10** and **26** was dissolved in a basic buffer (1.6 mL, 100 mM Na_2CO_3 and 50 mM Borate) and degased in a 15 mL Falcon tube with argon. To the degassed reaction mixture (500 μl) was added soluble Fe^{2+} (0.0005 eq.) and DTT (2.8 mg, 18.2 μmol, 1.5 eq.). The tube was sealed with a PTFE sealing tape and shaked for 4 h at 100 °C in an Eppendorf ThermoMixer®. After 4 h a carbonate solution (0.5 mL, 500 mM) was added and the reaction continued for another 20 h. After cooling to rt, it was centrifuged and a sample (20 μL) was removed and diluted with H_2O to 0.5 ml. This diluted sample was used for LC-MS analysis according to the general information.

(1R,2R,3R,4S)-tetrahydro-2H-pyran-2,3,4,5-tetrayl tetraacetate (30)
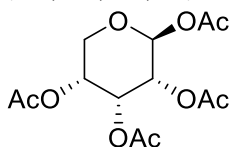
D-ribose (5.00 g, 33.3 mmol) was dissolved in pyridine (20 mL) and cooled to 0°C in an ice water bath. Acetic anhydride (20 ml, 212 mmol) was added and stirred at 0°C overnight. The mixture was poured into ice cold water (200 ml). The solid was filtered off and the crude product was crystallized from a mixture of MeOH and H_2O to obtain the pure product as colorless crystals (5.22 g, 16.4 mmol, 49%).

^{1}H NMR (400 MHz, CDCl$_3$) δ (ppm) = 6.02 (d, ^3J = 4.8 Hz, 1H, HC1), 5.47 (t, ^3J = 3.4 Hz, 1H, HC3), 5.19 – 5.11 (m, 1H, HC4), 5.05 – 5.00 (m, 1H, HC2), 4.01 (dd, ^2J = 12.4 Hz, ^3J = 3.4 Hz, 1H, H$_a$C5), 3.90 (dd, ^2J = 12.4 Hz, ^3J = 5.7 Hz, 1H, H$_b$C5), 2.12 (s, 3H, CH$_3$), 2.09 (s, 3H, CH$_3$), 2.09 (s, 3H, CH$_3$), 2.08 (s, 3H, CH$_3$). **^{13}C NMR** (101 MHz, CDCl$_3$) δ (ppm) = 170.0 (CO), 169.9 (CO), 169.6 (CO), 168.9 (CO), 91.0 (C1), 67.40 (C2), 66.3 (C3), 66.2 (C4), 62.8 (C5), 21.0 (CH$_3$), 20.9 (CH$_3$), 20.8 (CH$_3$), 20.8 (CH$_3$).

(1'R,2'R,3'R,4'S)-2-(2,4-Dioxo-3,4-dihydropyrimidin-1(2H)-yl)tetrahydro-2H-pyran-3,4,5-triyl triacetate (31)
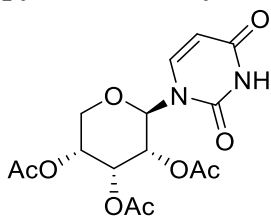

Uracil (269 mg, 2.40 mmol) was suspended in dry MeCN (14 ml) under inert atmosphere. The mixture was refluxed and bis(trimethylsilyl)acetamid (1.26 mL, 1.05 mg, 5.15 mmol) was added. After the mixture became clear, a solution containing tetraacetyl-β-D-ribose **30** (636 mg, 2.00 mmol, 0.8 eq.) and TMSOTf (0.54 mL ,667 mg, 3.00 mmol) in dry MeCN was added. The reaction was further refluxed for 8 h. After cooling to rt, the reaction was quenched with sat. NaHCO$_3$ (20 ml) and the aqueous phase

extracted with EtOAc (5 x 25 ml). The combined organic layers were dried over $MgSO_4$, filtered and the solvent removed *in vacuo*. The crude product was purified by flash column chromatography (DCM/MeOH 97:3) to obtain the pure compound as a yellowish solid (655 mg, 1.77 mmol, 89%).

mp: 164 °C. **^{1}H NMR** (400 MHz, DMSO-d_6) δ (ppm) = 11.47 (s, 1H, HN3), 7.90 (d, ^3J = 8.2 Hz, 1H, HC6), 5.85 (d, ^3J = 9.7 Hz, 1H, HC1'), 5.70 (dd, ^3J = 8.1 Hz, ^4J = 1.5 Hz, 1H, HC5), 5.66 – 5.63 (m, 1H, HC3'), 5.49 (dd, ^3J = 9.8, 3.1 Hz, 1H, HC2'), 5.23 – 5.15 (m, 1H, HC4'), 3.99 – 3.92 (m, 1H, H_aC5'), 3.85 (dd, ^2J = 11.0 Hz, ^3J = 5.5 Hz, 1H, H_bC5'), 2.19 (s, 3H, CH$_3$), 1.98 (s, 3H, CH$_3$), 1.92 (s, 3H, CH$_3$). **^{13}C NMR** (101 MHz, DMSO-d_6) δ (ppm) = 170.0 (CO), 169.3 (CO), 169.0 (CO), 162.8 (C4), 150.6 (C2), 140.7 (C6), 102.7 (C5), 77.7 (C1'), 67.7 (C3'), 66.5 (C2'), 65.5 (C4'), 62.7 (C5'), 20.5 (CH$_3$), 20.5 (CH$_3$), 20.3 (CH$_3$). **HRMS** (ESI+): calc.: [C$_{15}$H$_{19}$N$_2$O$_9$]$^+$ 371.1090, found: 371.1085 [M+H]$^+$. **IR** (cm^{-1}): $\tilde{\nu}$ = 3066 (vw), 2822 (vw), 2360 (vw), 1747 (s), 1692 (s), 1453 (w), 1371 (s), 1305 (w), 1212 (vs), 1163 (m), 1121 (w), 1079 (s), 1041 (s), 986 (m), 952 (m), 882 (w), 813 (m), 771 (w), 718 (w).

β-ᴅ-Ribopyranosyl-uracil (12d)
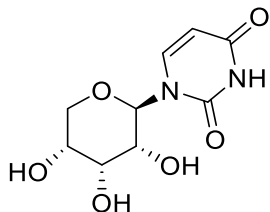
Nucleoside **31** (56 mg, 0.151 mmol) was dissolved in methanolic ammonia (4 ml, 1 M) and stirred for 19 h at rt. The solvent was removed *in vacuo* and the crude product was purified by flash column chromatography (DCM/MeOH 4:1) to obtain the pure product as a colorless solid (28.0 mg, 0.115 mmol, 76%). For LC-MS measurements, a fraction of the product was further purified by reversed phase HPLC.

mp: 220 °C (decomp.). **^{1}H NMR** (599 MHz, DMSO-d_6) δ (ppm) = 11.25 (s, 1H, HN3), 7.66 (d, ^3J = 8.1 Hz, 1H, HC6), 5.60 (d, ^3J = 8.1 Hz, 1H, HC5), 5.58 (d, ^3J = 9.4 Hz, 1H, HC1'), 5.11 (br, 1H, OH), 5.09 (br, 1H, OH), 4.84 (br, 1H, OH), 3.97 (d, ^3J = 3.2 Hz, 1H, HC3'), 3.68 (d, J = 9.5 Hz, 1H, HC2'), 3.63 (ddd, ^3J = 7.4, 6.0, 2.3 Hz, 1H, HC4'), 3.58 – 3.53 (m, 2H, H_aC5', H_bC5'). **^{13}C NMR** (101 MHz, DMSO-d_6) δ (ppm) = 163.0 (C4), 151.1 (C2), 141.4 (C6), 101.67 (C5), 79.6 (C1'), 71.2 (C3'), 67.6 (C2'), 66.4 (C4'), 65.2 (C5'). **HRMS** (ESI+): calc.: [C$_9$H$_{13}$N$_2$O$_6$]$^+$ 245.0768, found: 245.0768 [M+H]$^+$. **IR** (cm^{-1}): $\tilde{\nu}$ = 3347 (w), 2357 (vw), 2336 (vw), 1675 (vs), 1363 (w), 1391 (w), 1272 (m), 1250 (m), 1197 (m), 1084 (vs), 1042 (vs), 975 (m), 918 (w), 859 (w), 813 (m), 779 (w), 689 (m), 667 (m).

(1'R,2'S,3'S,4'R)-6-(2,4-Dioxo-3,4-dihydropyrimidin-1(2H)-yl)-2,2-dimethyltetrahydro-4H-[1,3]dioxolo[4,5-c]pyran-7-yl acetate (32)
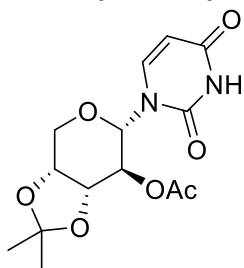
Uracil (224 mg, 2.00 mmol, 1.00 eq.) was suspended in dry MeCN (16 ml) under inert atmosphere. Bis(trimethylsilyl)acetamid (1.26 ml, 1.05 g, 5.00 mmol, 2.50 eq.) was added and stirred at 40 °C until the mixture became clear. TMSOTf (0.50 ml, 0.62 mg, 2.80 mmol, 1.40 eq.) was added. 1,2-O-acetate-3,4-O-isopropylidene-D-arabinose(*44*) (716 mg, 2.60 mmol, 1.30 eq.) was separately dissolved in dry MeCN (5 ml) and slowly added to the reaction mixture within 30 min. After stirring 2 h at 40 °C, the reaction was quenched with sat. $NaHCO_3$ (20 ml) and extracted with DCM (3 x 25 ml). The combined organic layers were washed with sat. NaCl (30 ml), dried over Na_2SO_4, filtered and the solvent removed *in vacuo*. The product was purified by flash column chromatography (iHex/acetone, 7:3 → 1:1) to yield the product as a colorless solid (565 mg, 1.73 mmol, 87%).

mp: 225 °C; **^{1}H NMR** (400 MHz, $CDCl_3$) δ (ppm) = 8.54 (s, 1H, HN3), 7.43 (d, ^3J = 8.2 Hz, 1H, HC6), 5.78 (dd, ^3J = 8.2 Hz, ^4J 2.3 Hz, 1H, HC5), 5.56 (d, ^3J = 9.4 Hz, 1H, HC1'), 5.10 (dd, ^3J = 9.4, 7.0 Hz, 1H, HC3'), 4.40 (d, ^2J = 13.9 Hz, 1H, H_aC5'), 4.34 (dd, J = 7.1, 5.4 Hz, 1H,HC2'), 4.31 – 4.26 (m, 1H, HC4'), 3.98 (dd, ^2J = 13.9, 2.4 Hz, 1H, H_b5'), 2.06 (s, 3H, CH_3), 1.59 (s, 3H, CH_3), 1.39 (s, 3H, CH_3). **^{13}C NMR** (101 MHz, $CDCl_3$) δ (ppm) = 170.0 (CO), 162.5 (C4), 150.4 (C2), 139.9 (C6), 110.8 (C_q), 103.3 (C5), 80.4 (C1'), 76.5 (C2'), 73.3 (C4'), 71.1 (C3'), 66.3 (C5'), 27.9 (CH_3), 26.2 (CH_3), 20.8 (CH_3). **HRMS** (ESI+): calc.: $[C_{14}H_{19}N_2O_7]^+$ 327.1187, found: 327.1188 $[M+H]^+$. **IR** (cm^{-1}): $\tilde{\nu}$ = 2985 (vw), 2882 (vw), 2359 (vw), 2053 (vw), 1741 (m), 1711 (s), 1675 (vs), 1470 (w), 1426 (w), 1375 (m), 1296 (m), 1249 (m), 1218 (vs), 1170 (w), 1130 (s), 1051 (vs), 967 (w), 889 (w), 847 (m), 797 (m), 761 (w), 686 (w).

1-((1'R,2'S,3'S,4'R)-7-Hydroxy-2,2-dimethyltetrahydro-4H-[1,3]dioxolo[4,5-c]pyran-6-yl)pyrimidine-2,4(1H,3H)-dion (33)
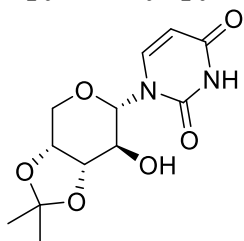

Nucleoside **32** (355 mg, 1.09 mmol) was dissolved in methanolic ammonia (14 ml, 1 M) and kept at rt for 20 h. The solvent was removed *in vacuo* and the crude product was purified by flash column chromatography (DCM/MeOH, 92:8) to obtain the product as colorless solid (284 mg, 1.00 mmol, 92%).

mp: 220 °C (decomp.). **¹H NMR** (400 MHz, DMSO-d_6) δ (ppm) = 11.36 (s, 1H, HN3), 7.65 (d, ^3J = 8.1 Hz, 1H, HC6), 5.64-5.59 (m, 2H, HC5, HO), 5.26 (d, ^3J = 9.7 Hz, 1H, HC1'), 4.23 – 4.18 (m, 1H, HC4'), 4.15 (d, ^2J = 13.5 Hz, 1H, H$_a$C5'), 4.11 (dd, ^3J = 7.0, 5.5 Hz, 1H, HC3'), 3.92 (dd, ^2J = 13.5 Hz, ^3J = 2.6 Hz, 1H, H$_b$C5'), 3.71 – 3.63 (m, 1H, HC2'), 1.49 (s, 4H, CH$_3$), 1.29 (s, 4H, CH$_3$). **¹³C NMR** (101 MHz, DMSO-d_6) δ (ppm) = 163.0 (C4), 151.0 (C2), 141.3 (C6), 108.7 (C$_q$), 102.0 (C5), 81.9 (C1'), 79.1 (C3'), 73.3 (C4'), 69.7 (C2'), 65.3 (C5'), 28.0 (CH$_3$), 26.2 (CH$_3$). **HRMS** (ESI+): calc.: [C$_{12}$H$_{17}$N$_2$O$_6$]$^+$ 285.1081, found: 285.1082 [M+H]$^+$. **IR** (cm^{-1}): $\tilde{\nu}$ = 3378 (w), 2989 (w), 2888 (vw), 2827 (vw), 2360 (vw), 1678 (vs), 1623 (m), 1469 (w), 1416 (w), 1392 (m), 1372 (m), 1336 (w), 1288 (m), 1275 (w), 1249 (s), 1216 (s), 1202 (s), 1167 (w), 1138 (s), 1108 (m), 1086 (vs), 1046 (s), 1022 (m), 975 (m), 958 (m, 936 (w), 874 (s), 846 (s), 826 (m), 796 (m), 780 (w), 761 (s), 732 (m), 684 (m).

1-((1'R,2'R,3'S,4'R)-7-Hydroxy-2,2-dimethyltetrahydro-4H-[1,3]dioxolo[4,5-c]pyran-6-yl)pyrimidine-2,4(1H,3H)-dion (34)
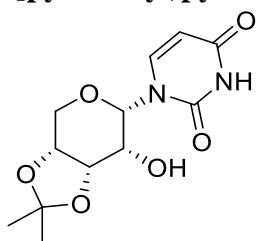
Nucleoside **33** (150 mg, 0.53 mmol) was dissolved in DCM (8 ml) together with Dess-Martin Periodinan (336 mg, 0.79 mmol) and NaHCO$_3$ (89 mg, 1.06 mmol). The reaction mixture was reacted for 2 h at 45 °C and quenched with solid Na$_2$S$_2$O$_3$ (0.55 g) together with sat. NaHCO$_3$ (5 ml). It was rigorously stirred until the organic phase became clear. The organic layer was separated and the aqueous layer was extracted with DCM (5 x 15 ml) and EtOAc (5 x 20 ml). The combined organic layers were dried over MgSO$_4$, filtered and the solvent removed *in vacuo*. The crude product was dissolved in a mixture of DCM/EtOAc/MeOH (2:1:1, 10 mL) and NaBH$_4$ (35 mg, 0.93 mmol) was added. The mixture was stirred for 1 h at 0 °C. The solvent was removed *in vacuo*. The residue was dissolved in EtOAc (20 ml) and washed with sat. NaCl (30 ml). The aqueous phase was extracted with EtOAc (8 x 25 ml). The combined organic layers were dried over MgSO$_4$, filtered and the solvent removed *in vacuo*. The crude product was purified by flash column chromatography (DCM/MeOH, 96:4) to obtain the product as a colorless solid (60 mg, 0.21 mmol, 40%).

mp: 205 °C (decomp.). **¹H NMR** (400 MHz, DMSO-d_6) δ (ppm) = 11.32 (s, 1H, HN3), 7.79 (d, ^3J = 8.1 Hz, 1H, HC6), 5.64 (d, ^3J = 3.0 Hz, 1H, HC1'), 5.56 (d, ^3J = 8.1 Hz, 1H, HC5), 5.40 (d, ^3J = 5.9 Hz, 1H, OH), 4.34 (dd, ^3J = 6.7, 4.5 Hz, 1H, HC3'), 4.24 – 4.19 (m, 1H, HC4'), 4.06 (dd, ^2J = 12.6 Hz, ^3J = 3.1 Hz, 1H, H$_a$C5'), 3.95 (dd, ^2J = 12.7 Hz, ^3J = 3.9 Hz, 1H, H$_b$C5'), 3.91 – 3.87 (m, 1H, HC2'), 1.46 (s, 3H, CH$_3$), 1.30 (s, 3H, CH$_3$). **¹³C NMR** (101 MHz, DMSO-d_6) δ (ppm) = 163.2 (C4), 150.3 (C2), 143.2 (C6), 109.1 (C$_q$), 100.0 (C5), 80.2 (C1'), 72.8 (C3'), 70.8 (C4'), 65.4 (C5'), 64.60 (C2'), 26.0 (CH$_3$), 25.5. (CH$_3$). **HRMS** (ESI+): calc.: [C$_{12}$H$_{17}$N$_2$O$_6$]$^+$ 285.1081, found: 285.1081 [M+H]$^+$. **IR** (cm^{-1}): $\tilde{\nu}$ = 2989 (vw), 2890 (vw), 2359 (vw), 2215 (vw), 1708 (s), 1674

(vs), 1454 (w), 1425 (w), 1381 (m), 1211 (s), 1155 (m), 1126 (s), 1084 (s), 1064 (vs), 1042 (vs), 991 (w), 882 (w), 846 (m), 814 (m), 763 (m), 737 (m), 678 (w).

α-D-Ribopyranosyl-Uracil (α-p-U, 12c)
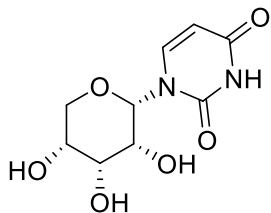
Nucleoside **34** was dissolved in 70% acetic acid (5 ml) and stirred for 5 h at 60 °C. The solvent was removed *in vacuo* and remaining AcOH was co-evaporated with EtOH (2 x 30 ml) and MeCN (3 x 30 ml). The crude product was purified by flash column chromatography (DCM/MeOH 88:12) to obtain the product as white solid (32.0 mg, 0.151 mmol, 83%). For LC-MS measurements, a fraction of the product was further purified by reversed phase HPLC.

mp: 243 °C (decomp.) **^{1}H NMR** (599 MHz, DMSO-d_6) δ (ppm) = 11.34 (s, 1H, HN3), 7.70 (d, ^3J = 8.2 Hz, 1H, HC6), 5.57 (d, ^3J = 8.1 Hz, 1H, HC5), 5.47 (d, ^3J = 1.2 Hz, 1H, HC1'), 5.27 (br, 1H, C2'OH), 5.17 – 5.12 (br, 1H, C3'OH), 5.10 (br, 1H, C4'OH), 3.96 (dd, ^2J = 12.4 Hz, ^3J = 1.6 Hz, 1H, H$_a$C5'), 3.75 (d, ^2J = 12.2 Hz, 1H, H$_b$C5'), 3.72 (d, ^3J = 7.4 Hz, 1H, HC2'), 3.70 – 3.66 (m, 2H, HC3', HC4'). **^{13}C NMR** (101 MHz, DMSO-d_6) δ (ppm) = 163.1 (C4), 150.0 (C2), 142.5 (C6), 100.1 (C5), 81.6 (C1'), 70.9 (C2'), 70.3 (C5'), 68.6 (C4'), 67.2 (C3'). **HRMS** (ESI+): calc.: [C$_9$H$_{13}$N$_2$O$_6$]$^+$ 245.0768, found: 245.0768 [M+H]$^+$. **IR** (cm^{-1}): $\tilde{\nu}$ =3359 (w), 3295 (w), 2934 (vw), 1769 (vw), 1716 (w), 1692 (m), 1665 (s), 1461 (m), 1432 (w), 1398 (w), 1385 (w), 1373 (w), 1322 (vw), 1295 (m), 1251 (m), 1195 (w), 1159 (w), 1110 (m), 1084 (vs), 996 (w), 968 (w), 911 (w), 889 (w), 834 (w), 818 (s), 769 (vs), 714 (s), 670 (s).

Synthesis pathway for α-furanosyl-uridine

(1'S,2'R,3'S,4'R)-2-amino-5-(hydroxymethyl)-3a,5,6,6a-tetrahydrofuro[2,3-d]oxazol-6-ol (35)
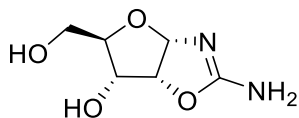

D-Ribose (14.4 g, 96 mmol) and cyanamide (8.06 g, 192 mmol) were dissolved in aqueous ammonia (16 ml, 1M) in a pressure tube. The mixture was heated at 30 °C until the solution became clear. The reaction was further stirred at rt until a precipitate started to form. The reaction was heated for 30 min at 60 °C and the solvent removed *in vacuo*. The residue was taken up in hot MeOH (32 ml) and filtrated immediately. The warm filtrate was kept at -20 °C overnight. The yellowish solid was filtered off and washed with MeOH and Et$_2$O to obtain the pure product as a colorless solid (12.6 g, 72.3 mmol, 75%).[47]

The analytical data is in agreement with reported literature.[48]

^{1}H NMR (400 MHz, DMSO-d_6) δ (ppm) = 6.14 (d, ^3J = 1.8 Hz, 2H), 5.57 – 5.12 (m, 1H), 4.29 (dd, ^3J = 18.4, 1.9 Hz, 2H), 2.00 – 1.78 (m, 2H), 1.74 – 1.66 (m, 1H), 1.51

– 1.29 (m, 2H). ^{13}C NMR (101 MHz, DMSO-d_6) δ (ppm) = 164.0, 98.1, 80.9, 77.8, 71.1, 60.4.

(1'S,2'R,3'S,4'R)-3-Hydroxy-2-(hydroxymethyl)-2,3,3a,9a-tetrahydro-6H-furo[2',3':4,5]oxazolo[3,2-a]pyrimidin-6-on (36)
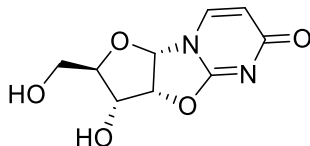
Compound **35** (10.0 g, 75.4 mmol) and methyl propiolate (9.60 g, 9.65 mL, 114 mmol) were dissolved in H_2O (130 mL) and stirred at 100 °C for 30 min. The solvent was removed *in vacuo* and the residue taken up in hot MeOH (65 ml). The solution was filtered hot and the filtrate kept at -20 °C for 48 h. The formed yellow crystals were filtered off to obtain the pure product (6.21 g, 27.5 mmol, 48%).[47] The analytical data is in agreement with reported literature.[49]

^{1}**H NMR** (400 MHz, DMSO-d_6) δ (ppm) = 7.85 (d, ^3J = 7.4 Hz, 1H), 6.20 (d, ^3J = 5.3 Hz, 1H), 5.88 (d, ^3J = 7.4 Hz, 1H), 5.77 (d, ^3J = 6.8 Hz, 1H), 5.23 (t, ^3J = 5.4 Hz, 1H), 4.91 – 4.86 (m, 1H), 4.05 (ddd, ^3J = 9.1, 6.8, 5.4 Hz, 1H), 3.69 (ddd, ^2J = 12.3 Hz, ^3J = 4.9, 2.0 Hz, 1H), 3.56 (ddd, ^3J = 9.2, 5.0, 1.9 Hz, 1H), 3.50 – 3.42 (m, 1H). ^{13}**C NMR** (101 MHz, DMSO-d_6) δ (ppm) = 171.2, 160.8, 137.0, 108.9, 88.7, 81.5, 80.8, 69.7, 59.5.

α-furanosyl-uracil (12a)
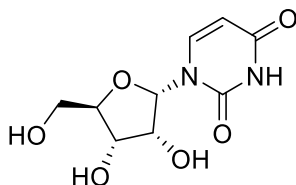
Compound **36** (1.0 g, 4.40 mmol) dissolved in aqueous HCl (2.2 ml, 0.2 M) was refluxed for 2 h. The solvent was removed *in vacuo* and the residue was taken up in H_2O. The solution was neutralized until pH ~6 with Dowex 1X8. It was filtered and the resin was washed with H_2O. The filtrate was freeze dried to obtain the product as a colorless powder (1.02 g, 4.18 mmol, 95%). For LC-MS analysis, a small fraction of the product was further purified by reversed phase HPLC.

mp: 202 °C (decomp.). ^{1}**H NMR** (400 MHz, DMSO-d_6) δ (ppm) = 11.18 (s, 1H, HN3) 7.61 (d, ^3J = 8.1 Hz, 1H, HC6), 6.01 (d, ^3J = 4.6 Hz, 1H, HC1'), 5.56 (d, ^3J = 8.1 Hz, 1H, HC5), 5.49 (br, 1H, OH), 5.12 (br, 1H, OH), 4.80 (d, ^3J = 9.0 Hz, 1H, OH), 4.16 (t, ^3J = 4.5 Hz, 1H, HC2'), 4.06 – 3.98 (m, 2H, HC3', HC4'), 3.58 (dd, ^2J = 12.0 Hz, ^3J = 2.7 Hz, 1H, H_aC5), 3.42 (dd, ^2J = 12.2 Hz, ^3J = 4.1 Hz, 1H, H_bC5). ^{13}**C NMR** (101 MHz, DMSO-d_6) δ (ppm) = 163.3 (C4), 150.6 (C2), 142.8 (C6), 99.8 (C5), 85.1 (C1'), 84.0 (C4'), 70.4 (C3'), 70.3 (C2'), 61.2 (C7). **HRMS** (ESI+): calc.: [$C_9H_{13}N_2O_6$]$^+$ 245.0768, found: 245.0768 [M+H]$^+$. **IR** (cm^{-1}): $\tilde{\nu}$ = 3301 (w), 3058 (w), 2930 (w), 2805 (vw), 2342 (vw), 1659 (vs), 1463 (m), 1394 (m), 1269 (s), 1197 (m), 1096 (s), 1037 (vs), 1021 (vs), 990 (s), 927 (m), 857 (m), 806 (s), 763 (s), 718 (m).

Synthesis of α-furanosyl-cytidine(1'S,2'R,3'S,4'R)-2-(acetoxymethyl)-5-(2,4-dioxo-3,4-dihydropyrimidin-1(2H)-yl)tetrahydrofuran-3,4-diyl diacetate (37)
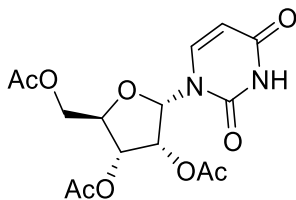
Compound **12a** (500 mg, 2.05 mmol) was dissolved in pyridine (5 ml) and acetic anhydride (5 ml) at 0 °C. The mixture was reacted for 18 h and the solvent removed *in vacuo*. It was co-evaporated with MeCN (20 ml). The residue was purified by flash column chromatography (DCM/MeOH 97:3) to afford the product as a colorless solid (611 mg, 1.65 mmol, 80%).

mp: 70 °C. **^{1}H NMR** (400 MHz, DMSO-d_6) δ(ppm) = 11.38 (s, 1H, HN3), 7.65 (d, ^3J = 8.2 Hz, 1H, HC6), 6.34 (d, ^3J = 4.7 Hz, 1H, HC1'), 5.64 (d, ^3J = 8.2 Hz, HC5), 5.54 (t, ^3J = 4.7 Hz, 1H, HC2'), 5.35 (dd, ^3J = 6.2, 5.1 Hz, 1H, HC3'), 4.66 – 4.60 (m, 1H, HC4'), 4.26 (dd, ^2J = 12.2 Hz, ^3J = 3.4 Hz, 1H, H$_a$C5'), 4.16 (dd, ^2J = 12.2 Hz, ^3J = 5.7 Hz, 1H, H$_b$C5'), 2.06 (s, 3H, CH$_3$), 2.03 (s, 3H, CH$_3$), 1.97 (s, 3H, CH$_3$). **^{13}C NMR** (101 MHz, DMSO-d_6) δ(ppm) = 170.1 (CO), 169.4 (CO), 168.8 (CO), 163.1 (C4), 150.2 (C2), 141.0 (C6), 100.9 (C5), 83.5 (C1'), 78.8 (C4'), 70.6 (C3') 69.8 (C2'), 63.1 (C5'), 20.6 (CH$_3$), 20.4 (CH$_3$), 20.1 (CH$_3$). **HRMS** (ESI+): calc.: $[C_{15}H_{18}N_2NaO_9]^+$ 393.0905, found: 393.0904 [M+Na]$^+$. **IR** (cm^{-1}): $\tilde{\nu}$ = 3059 (vw), 2159 (vw), 1743 (s), (1682 (vs), 1455 (w), 1371 (m), 1211 (vs), 1109 (s), 1075 (m), 1030 (s), 944 (w), 902 (w), 813 (m), 766 (w), 714 (w), 674 (vw).

α-furanosyl-cytidine (11a)
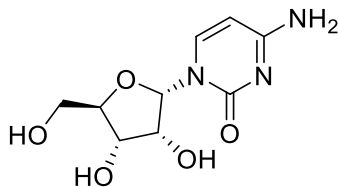
Compound **37** (100 mg, 0.27 mmol) was dissolved in dry DCM. It was added Et$_3$N (105 µL, 78.1 mg, 0.77 mmol), DMAP (6.00 mg, 0.05 mmol) and 2,4,6-TIPBS (164 mg, 0.54 mmol) and stirred for 20 h at rt. The reaction was quenched with sat. aqueous ammonia (6 ml) and further stirred for 3 h at rt. The solvent was removed *in vacuo* and residual water co-evaporated with MeCN (2 x 25 ml). The residue was purified by flash column chromatography (DCM/MeOH 88:12) and reversed phase HPLC to afford the product as a colorless solid (15 mg, 0.06 mmol, 23%)

mp: 190 °C. **^{1}H NMR** (400 MHz, DMSO-d_6) δ(ppm) = 7.52 (d, ^3J = 7.4 Hz, 1H, HC6), 7.05 (br, 1H, H$_a$N), 6.96 (br, 1H, H$_b$N), 6.01 (d, ^3J = 3.7 Hz, 1H, HC1'), 5.66 (d, ^3J = 7.4 Hz, 1H, HC5), 5.27 (s, 1H, OH), 4.97 (s, 1H, OH), 4.77 (s, 1H, OH), 4.07 – 4.01 (m, 2H, HC2', HC3'), 3.98 – 3.92 (m, 1H, HC4'), 3.61 (dd, ^2J = 12.1 Hz, ^3J = 2.6 Hz, 1H, H$_a$C5'), 3.42 (dd, ^2J = 12.2 Hz, ^3J = 4.6 Hz, 1H, H$_b$C5'). **^{13}C NMR** (101 MHz, DMSO-d_6) δ(ppm) = 165.6 (C4), 155.2 (C2), 143.1 (C6), 92.3 (C5), 85.6 (C1'), 83.1 (C4'), 70.6 (C2'), 70.1 (C3'), 61.1 (C5'). **HRMS** (ESI+): calc.: $[C_9H_{14}N_3O_5]^+$ 244.0928,

found: 244.0927 [M+H]$^+$. **IR** (cm^{-1}): $\tilde{\nu}$ = 3267 (w), 2360 (vs), 2222 (s), 1842 (m), 1589 (m), 1311 (w), 1210 (w), 1033 (m), 793 (m), 668 (vs).

Synthesis of α-pyranosyl-cytidine 4-amino-1-((1'R,2'S,3'S,4'R)-7-hydroxy-2,2-dimethyltetrahydro-4H-[1,3]dioxolo[4,5-c]pyran-6-yl)pyrimidin-2(1H)-on (38)
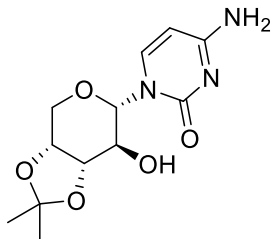
Compound **32** (143 mg, 0.44 mmol) was dissolved in dry DCM (9 ml). It was added triethylamine (118 mg, 162 ml, 1.60 mmol), DMAP (8 mg, 0.07 mmol, 0.15 eq.) and 2,4,6-TIPBS (265 mg, 0.88 mmol). The mixture was reacted for 72 h at rt and quenched with sat. ammonia in H$_2$O (3 ml). The reaction was further stirred for 5 h at rt. The solvent was removed *in vacuo* und residual H$_2$O was co-evaporated with MeCN (2 x 25 ml). The crude mixture was purified by flash column chromatography (DCM/MeOH 12:1 → 4:1, containing 0.1% Et$_3$N) to obtain the product as a white solid (67 mg, 0.21 mmol, 48%).

mp: 210 °C (decomp.). **^{1}H NMR** (400 MHz, DMSO-d_6) δ (ppm) = 7.54 (d, ^3J = 7.5 Hz, 1H, HC6), 7.23 (br, 1H, H$_a$N), 7.11 (br, 1H, H$_b$N), 5.71 (d, ^2J = 7.4 Hz, 1H, HC5), 5.41 (d, ^3J = 6.4 Hz, 1H, OH), 5.36 (d, ^3J = 9.8 Hz, 1H, HC1'), 4.22 – 4.18 (m, 1H, HC4'), 4.14 – 4.07 (m, 2H, H$_a$C5', HC3'), 3.85 (dd, ^2J = 13.6 Hz, ^3J = 2.5 Hz, 1H, H$_b$C5'), 3.67 – 3.57 (m, 1H, HC3'), 1.48 (s, 3H, CH$_3$), 1.29 (s, 3H, CH$_3$). **^{13}C NMR** (101 MHz, DMSO-d_6) δ (ppm) = 165.4 (C4), 155.5 (C2), 141.7 (C6), 108.5 (C$_q$), 94.2 (C5), 82.3 (C1'), 79.4 (C3'), 73.3 (C4'), 69.9 (C2'), 65.2 (C5'), 28.0 (CH$_3$), 26.2 (CH$_3$). **HRMS** (ESI+): calc.: [C$_{12}$H$_{18}$N$_3$O$_5$]$^+$ 284.1240, found: 284.1241 [M+H]$^+$. **IR** (cm^{-1}): $\tilde{\nu}$ = 3326 (w), 2932 (w), 2819 (vw), 2360 (vw), 1660 (vs), 1525 (vw), 1465 (m), 1395 (m), 1270 (s), 1203 (m), 1096 (s), 1039 (vs), 1022 (s), 928 (w), 869 (m), 808 (s), 763 (m), 719 (m).

α-pyranosyl-cytidine (11c)
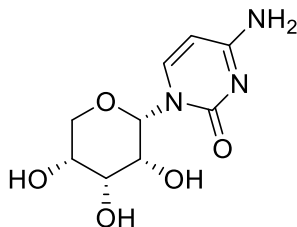
Compound **38** (35 mg, 0.12 mmol) was dissolved in MeCN (5.5 ml). Dess-Martin-Periodinan (104 mg, 0.25 mmol) was added and the reaction mixture was stirred for 3.5 h at rt. The reaction was quenched with Na$_2$S$_2$O$_3$ (500 mg) und NaHCO$_3$ (100 mg) and further stirred for 10 min. The mixture was filtered and the solvent removed *in vacuo*. The crude keto product was dissolved in DCM (3 mL), EtOAc (1.5 mL) und MeOH (1.5 mL). NaBH$_4$ (20 mg, 0.529 mmol) was added and stirred for 2.5 h at rt. The solvent

was removed *in vacuo*. The crude product was dissolved in 70% acetic acid (5 ml) and stirred for 5 h at 60 °C. The solvent was removed *in vacuo* and co-evaporated with EtOH (2 x 30 ml) and MeCN (3 x 30 ml). The crude mixture was purified by reversed phase HPLC to obtain the product as colorless solid (7.0 mg, 0.029 mmol, 24 %).

mp: 194 °C (decomp.). **^{1}H NMR** (400 MHz, DMSO-d_6) δ (ppm) = 7.61 (d, ^3J = 7.4 Hz, 1H, HC6), 7.18 (br, 1H, H$_a$N), 7.02 (br, 1H, H$_b$N), 5.67 (d, ^3J = 7.4 Hz, 1H, HC5), 5.47 (s, 1H, HC1'), 5.13 (d, ^3J = 6.0 Hz, 1H, OH), 5.10 (d, ^3J = 5.8 Hz, 1H, OH), 5.07 (d, ^3J = 7.7 Hz, 1H, OH), 3.95 (dd, ^2J = 12.2 Hz, ^3J = 1.8 Hz, 1H, H$_a$C5'), 3.75 – 3.63 (m, 4H, HC2, HC3, HC4, H$_b$C5').**^{13}C NMR** (101 MHz, DMSO-d_6) δ (ppm) = 165.5 (C4), 154.4 (C2), 143.1 (C6), 92.5 (C5), 82.3 (C1'), 70.6 (C2'), 70.3 (C5'), 68.7 (C4'), 67.4 (C3'). **HRMS** (ESI+): calc.: [C$_9$H$_{14}$N$_3$O$_5$]$^+$ 244.0928, found: 244.0927 [M+H]$^+$. **IR** (cm^{-1}): $\tilde{v}$ = 3217 (w), 2360 (vw), 1891 (vw), 1645 (s), 1598 (m), 1525 (w), 1481 (m), 1405 (m), 1299 (m), 1203 (m), 1158 (m), 1084 (vs), 1015 (s), 987 (s), 902 (m), 833 (m), 780 (vs), 752 (s), 668 (vs).

Synthesis of β-pyranosyl-cytidine β-pyranosyl-cytidine (11d)
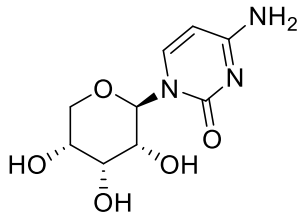
Nucleoside **31** (50.0 mg, 0.135 mmol) was dissolved in dry DCM. It was added NEt$_3$ (27.3 mg, 37.4 µL, 0.270 mmol), DMAP (1.7 mg, 0.014 mmol, 0.1 eq.) and 2,4,6-TIPBS (61.5 mg, 0.203 mmol) and stirred for 17 h at rt. The reaction was quenched with sat. ammonia in H$_2$O. The solvent was removed *in vacuo* and residual water was co-evaporated with MeCN (4 x 20 ml). The crude product was purified by reversed phase HPLC to obtain the pure product as a colorless solid (15 mg, 0.062 mmol, 46%).

mp: 180 °C. **^{1}H NMR** (599 MHz, DMSO-d_6) δ (ppm) = 7.54 (d, ^3J = 7.4 Hz, 1H, HC6), 7.16 (br, 1H, H$_a$N), 7.05 (br, 1H, H$_b$N), 5.70 (d, ^3J = 9.6 Hz, 1H, HC1'), 5.68 (d, J = 7.5 Hz, 1H, HC5), 5.01 (d, ^3J = 3.5 Hz, 1H, OH), 4.83 (d, ^3J = 7.2 Hz, 1H, OH), 4.78 (br, 1H, OH), 3.96 (s, 1H, HC3'), 3.64 – 3.57 (m, 2H, HC4', HC2'), 3.54 (d, ^2J = 10.2 Hz, 1H, H$_a$C5'), 3.50 (dd, ^2J = 10.3 Hz, ^3J = 5.0 Hz, 1H, H$_b$C5'). **^{13}C NMR** (101 MHz, DMSO-d_6) δ (ppm) = 165.3 (C4), 155.7 (C2), 141.8 (C6), 93.9 (C5), 79.8 (C1'), 71.2 (C3'), 68.0 (C2'), 66.7 (C4'), 65.2 (C5'). **HRMS** (ESI+): calc.: [C$_9$H$_{14}$N$_3$O$_5$]$^+$ 244.0928, found: 244.0927 [M+H]$^+$. **IR** (cm^{-1}): $\tilde{v}$ = 3426 (w), 3210 (m), 2922 (w), 1640 (vs), 1596 (vs), 1526 (m), 1489 (vs), 1400 (m), 1387 (m), 1368 (m), 1322 (w), 1300 (m), 1281 (m), 1269 (m), 1242 (m), 1224 (m), 1204 (s), 1132 (s), 1115 (m), 1094 (s), 1076 (s), 1039 (vs), 1018 (s), 991 (s), 970 (m), 800 (m), 781 (s), 660 (vs).

Synthesis of lüneburgite: Mg$_3$(H$_2$O)$_6$[B$_2$(OH)$_6$(PO$_4$)$_2$]

The synthesis was performed according to literature.(*50*) Magnesiumoxide (1 g, 25 mmol), dimagnesiumphosphate trihydrate (8.1 g, 46.5 mmol) and boric acid (9.2 g, 149 mmol) were refluxed in H$_2$O (200 ml) for 4 days. After cooling to rt, the colorless solid was filtered off to afford the product (9.5 g, 19.2 mmol, 83%). The mineral was analysed by XRD measurement to confirm the correct product (see Fig. S10).

Synthesis of struvite: MgNH$_4$PO$_4$ x 6H$_2$O

The synthesis was performed according to literature.(*51*) A solution of (NH$_4$)$_2$PO$_4$ (50 mL, 1 M, 50 mmol) was added to a solution of MgCl$_2$ (50 mL, 1M, 50 mmol). The mixture was stirred for 15 min at room temperature. The solid was filtered off and washed with water to afford the product as a white solid (8.1 g). The mineral was analysed by XRD measurement to confirm the correct product (see Fig. S11).
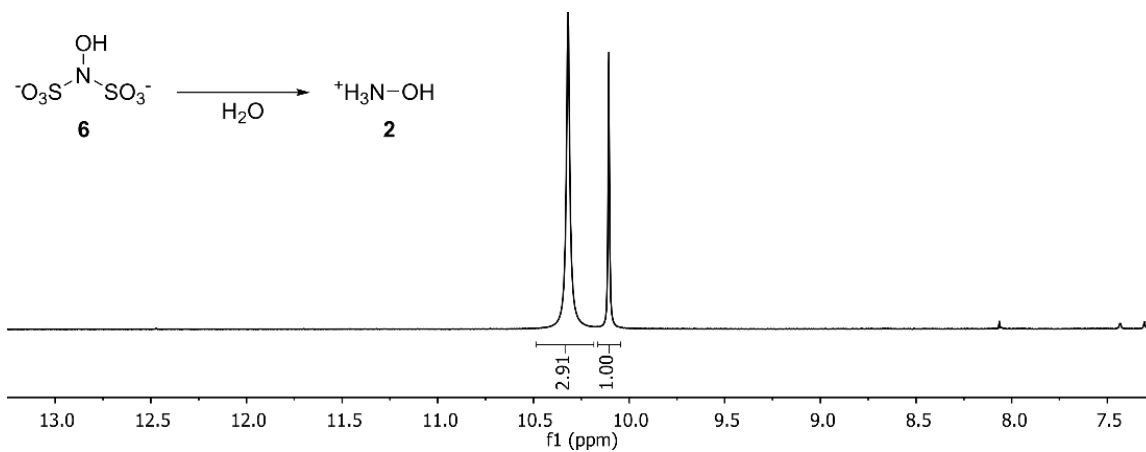
Fig. S1.

Hydrolysis of hydroxylamine disulfonate (**6**) affords hydroxylamine (**2**) as reveald by ^{1}H-NMR. Detailed information can be found in the aforementioned synthetic procedure.

a)

b)
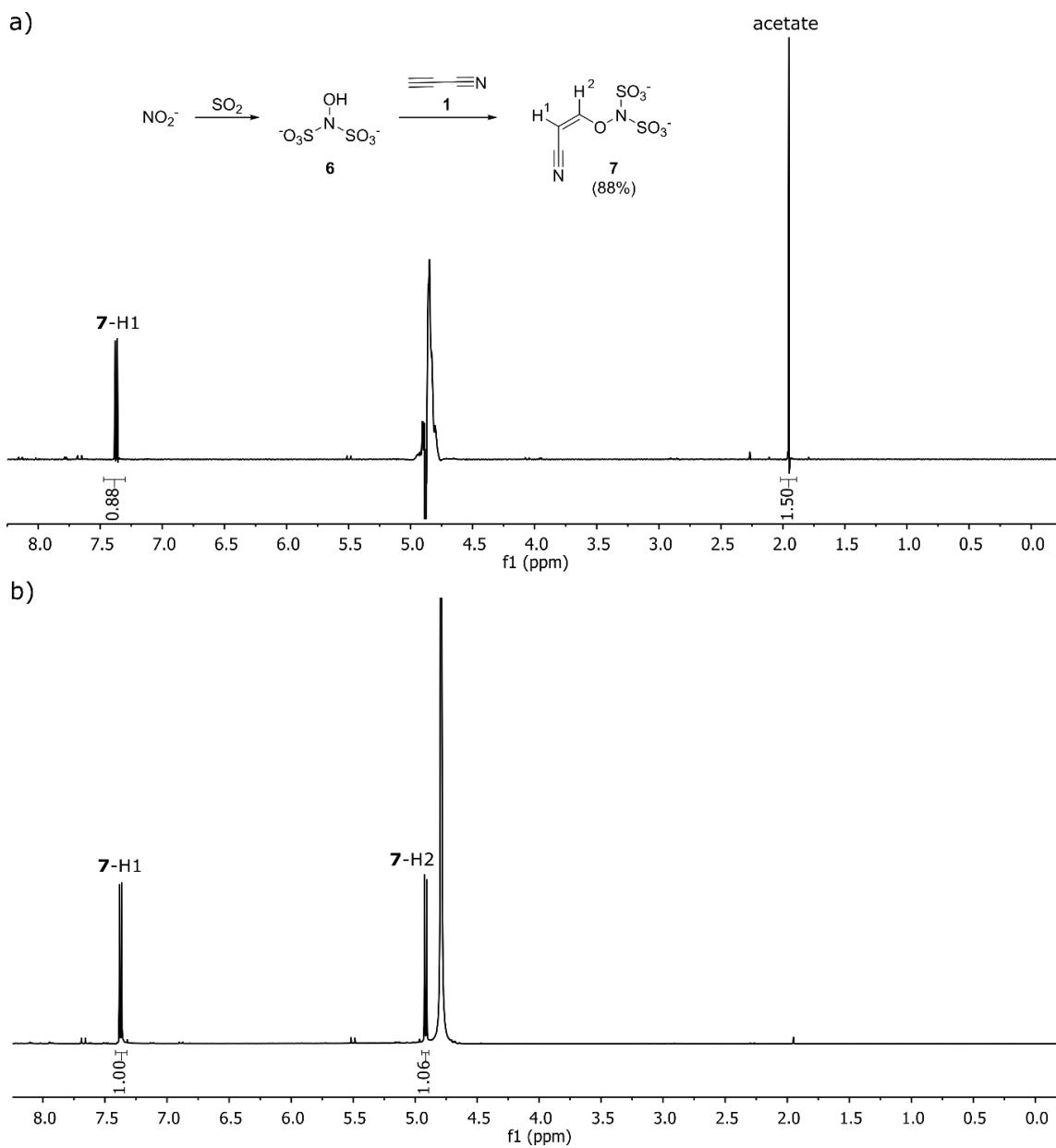

Fig. S2.
^{1}H NMR analysis for the formation of *cis*-**7**. a) Treatment of an aqueous nitrite solution with SO_2 afforded **6**, which further reacted with **1** to give adduct **7**. Detailed information can be found in the aforementioned procedure. ^{1}H-NMR spectroscopy in H_2O/D_2O (9:1) reveals formation *cis*-**7** (88%). Quantification was achieved using sodium acetate (0.5 eq) as reference standard. b) Since water suppression interferes with the H-2 signal of the *cis*-**7** isomer, we isolated and spectroscopically characterized the compound in D_2O.
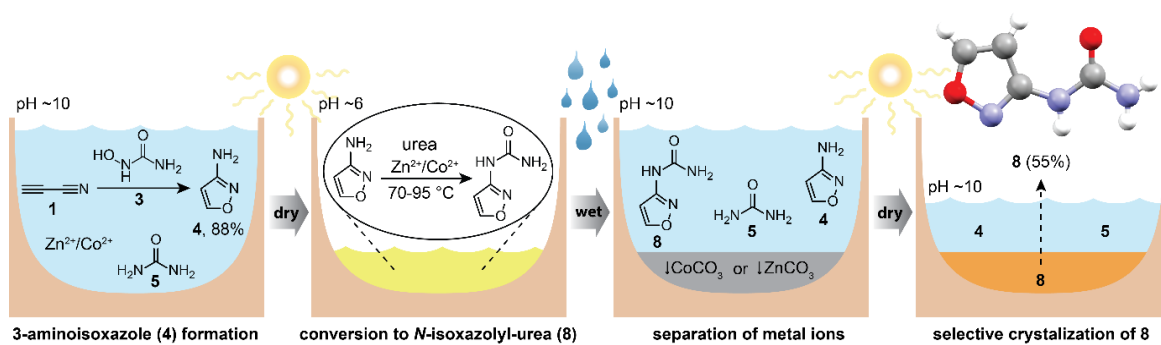
Fig. S3.

Plausible prebiotic scenario for the one-pot formation and enrichment of isoxazolylurea **8**.
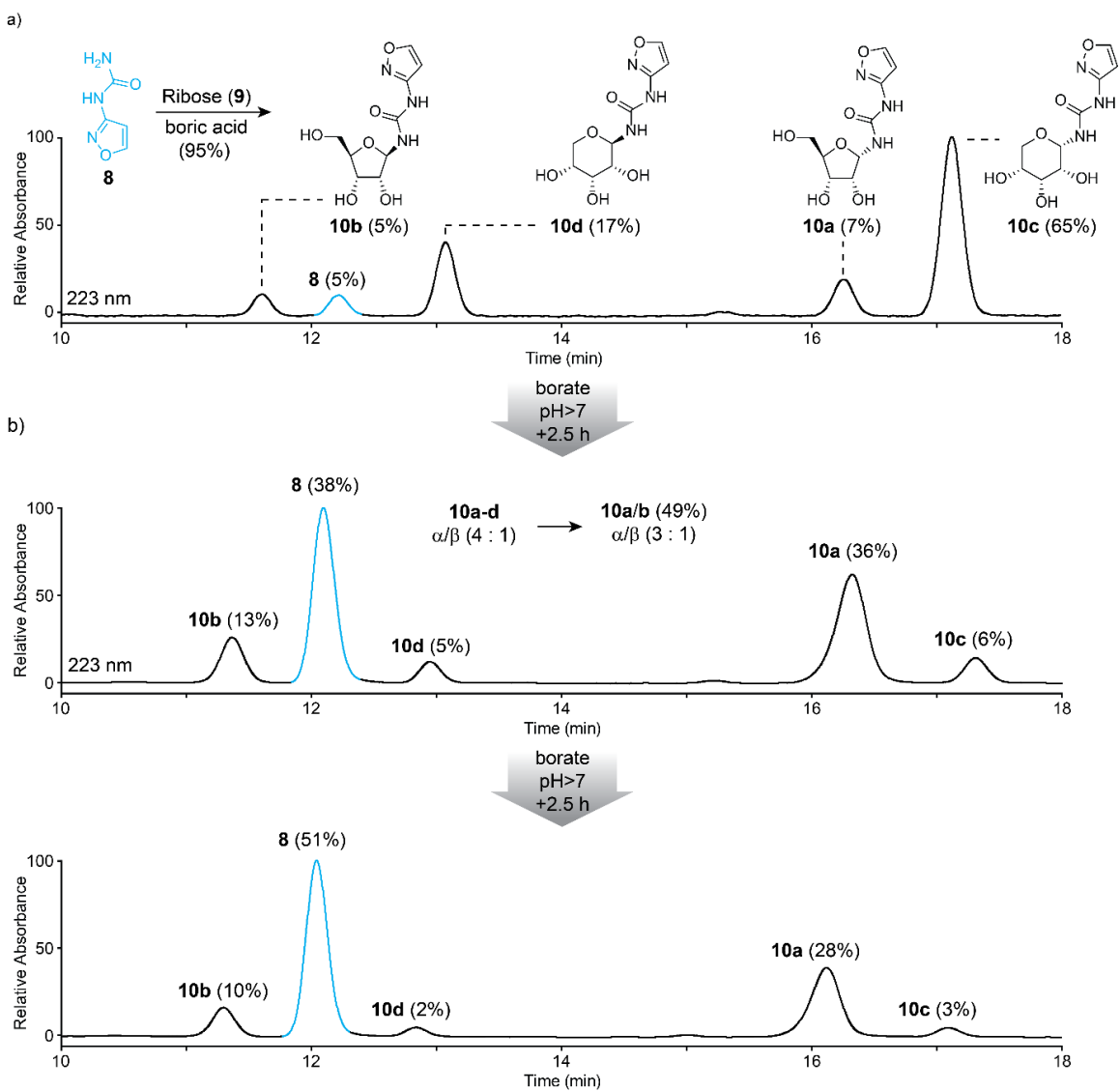
Fig. S4.

LC-MS analysis for the formation of **10a-d**. The UV-chromatograms at 223 nm are shown. a) Boric acid catalysed ribosylation of **8** affords the four expected α and β-anomers of isoxazolyl-urea as furanoside **10 a,b** or pyranoside **10c,d**. b) The mixture obtained in a) was heated in 125 mM borax at 95 °C for 2.5 h. Isomerization is also possible at lower temperature but with longer reaction time. The pyranoside products (**10c** and **d**) are converted into the furanoside products (**10a** and **b**). Further reaction gives **10a** and **b** as the only ribosides with only trace amounts of the pyranosides **10c** and **d** after 5 h.
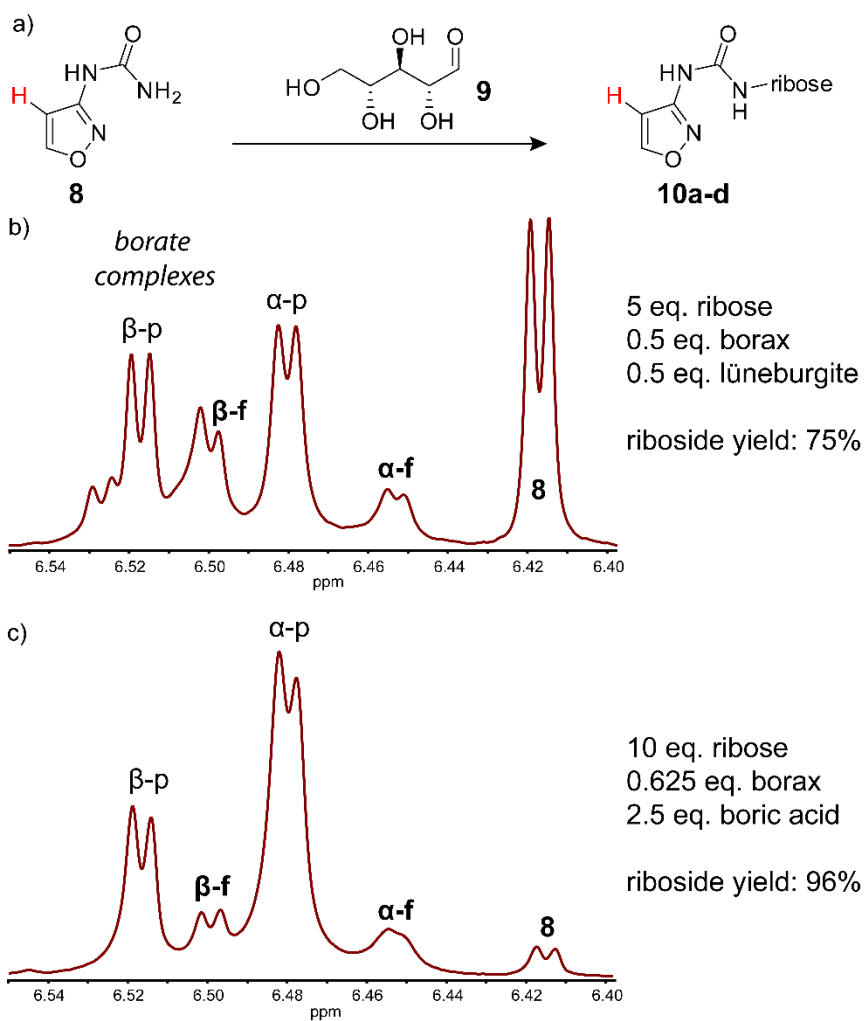
Fig. S5.

^{1}H-NMR in D₂O after **8** was reacted with ribose under different conditions. The ribosylated product **10a-d** is obtained as a mixture of α- and β-anomers as either furanoside (f) or pyranoside (p). The ^{1}H-NMR signals observed correspond to the proton labelled in red. The yields are relative to the starting material **8**. a) reaction scheme. b) the slightly basic conditions are expected to give borate complexes that are overlapping with the free nucleosides. c) more acidic conditions lead to higher degree of glycosylation and no borate complexes.
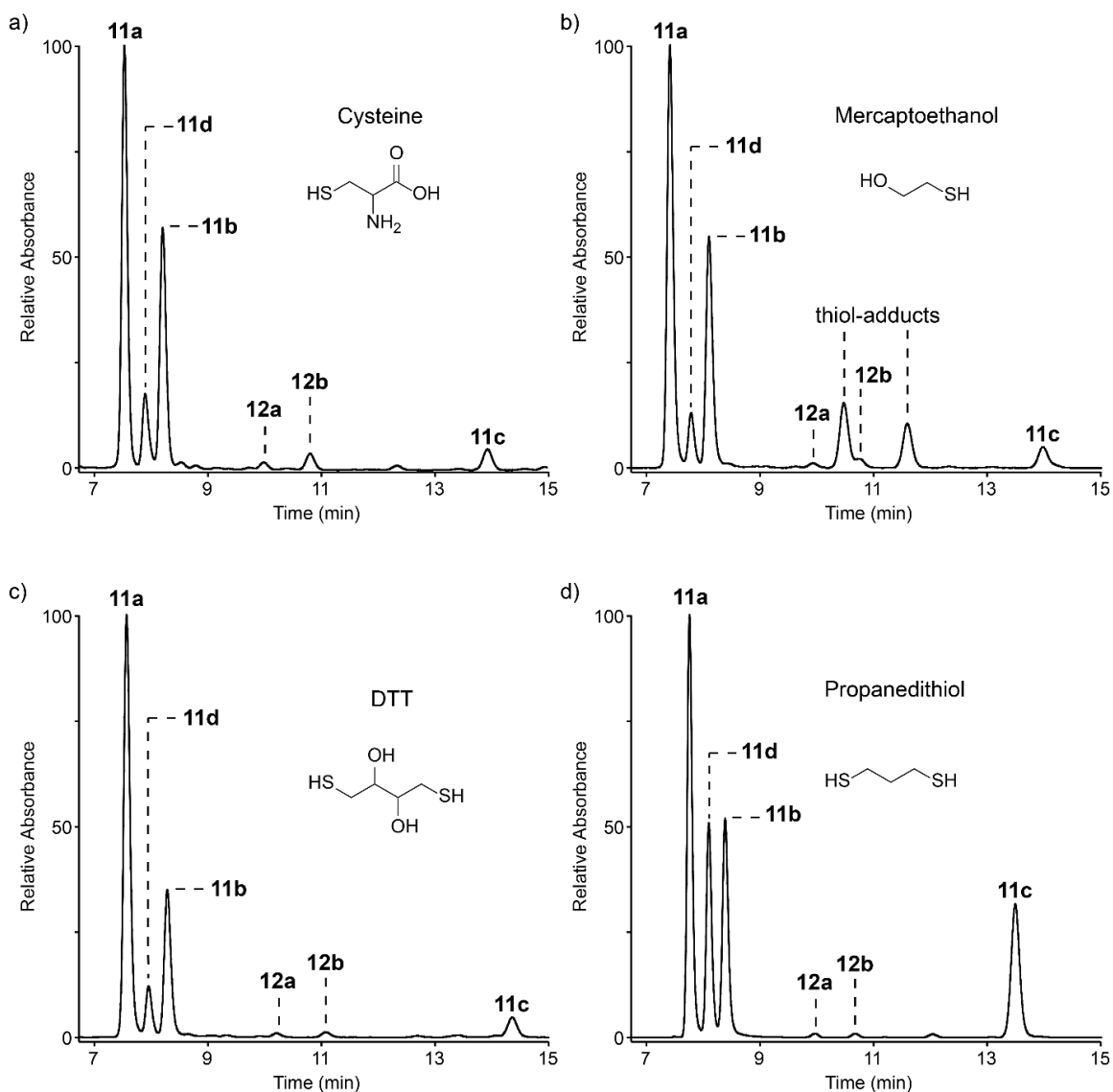
Fig. S6.

Cytidine **11a-d** and uridine **12a/b** formation in the presence of different thiols. All reductions were performed with 0.001 eq. of soluble Fe^{2+} in 100 mM sodium carbonate, 50 mM borate buffer (pH 9.7). Reduction in the presence of different thiols: a) cysteine, b) mercaptoethanol, c) dithiothreitol (DTT) and d) propanedithiol. e) table with calculated yields for **11a-d** and **12a/b**. For mercaptoethanol the overall yield is significantly lower, probably due to formation of thiol-adducts as labeled in b).
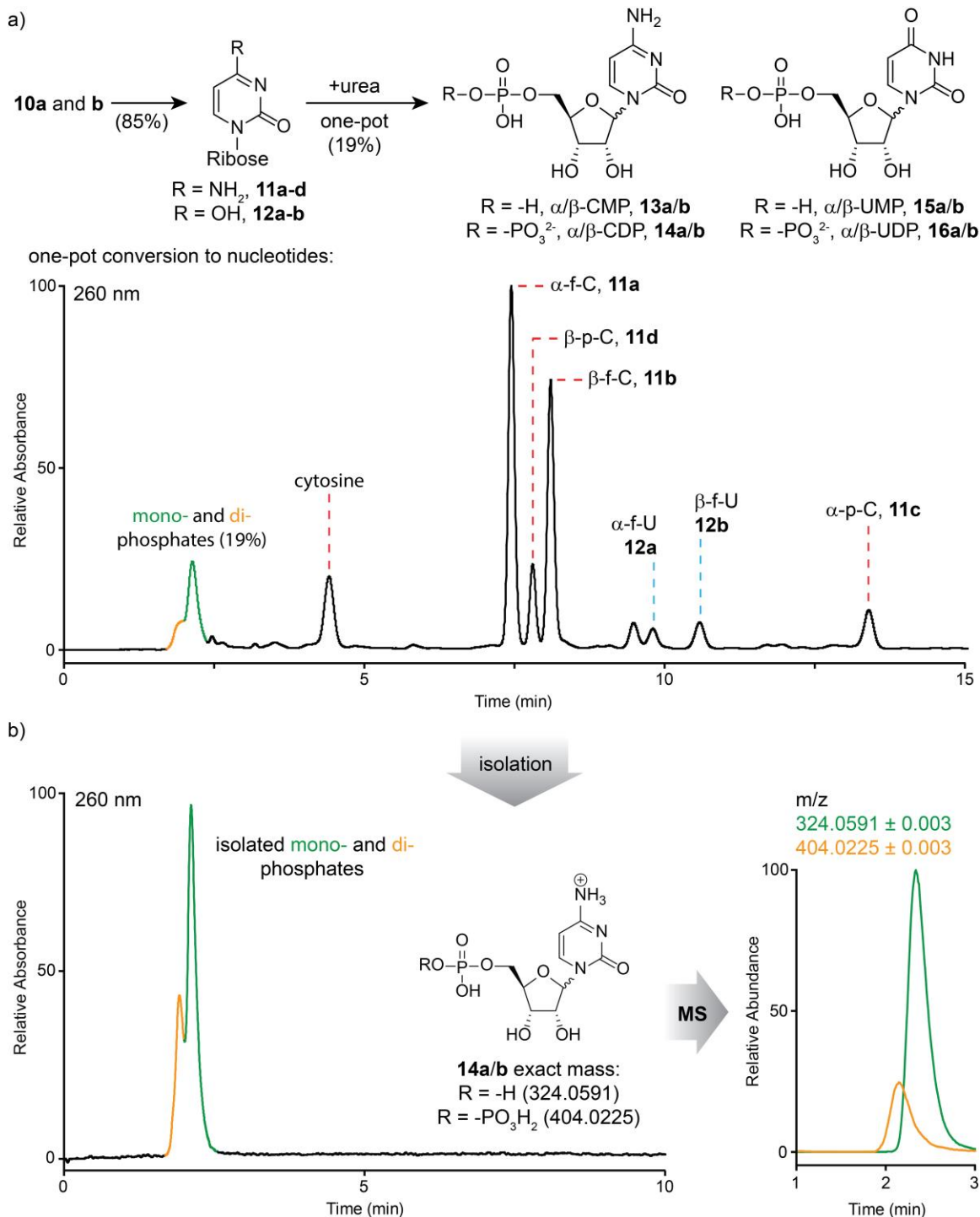
**Fig. S7.**
Prebiotic nucleotide synthesis in the presence of lueneburgite. a) Reaction scheme and full UV-chromatogram after nucleotide formation. An extract was shown in Fig. 5b in the main text. The yield was calculated relative to all cytidine isomers. The mono- (green) and di-phosphate (orange) peaks are highlighted. b) UV-chromatogram and corresponding mass (ESI+) for the isolated nucleotides.
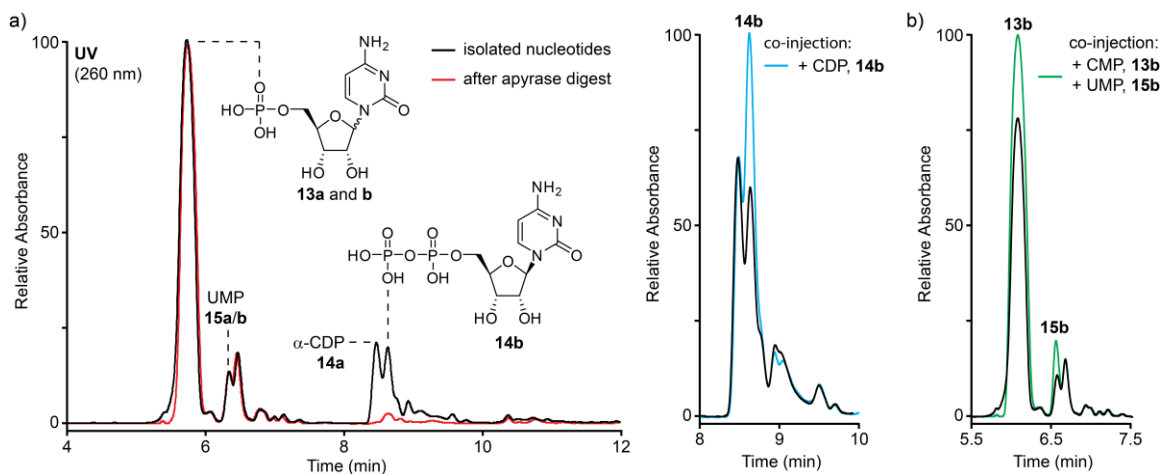
Fig. S8.

Confirmation of nucleotide structures from a prebiotic sample. a) LC-MS separation of phosphorylated nucleosides, isolated from a prebiotic reaction. The products were compared with a sample treated with apyrase. The di-phosphorylated peaks are clearly depleted in the treated sample (red line), proving the formation of pyrophosphates (left panel). Co-injection with 5'-cytidine-di-phosphate (**14b**, β-CDP) clearly confirmed formation of α- and β-CDP (right panel) . b) Co-injection of 5'-cytidine and 5'-uridine-mono-phosphate (**13b** and **15b**, β-CMP and β-UMP) confirmed the formation of **13b** and **15b**. The peaks represent mixtures of the inseparable α- and β-anomers.
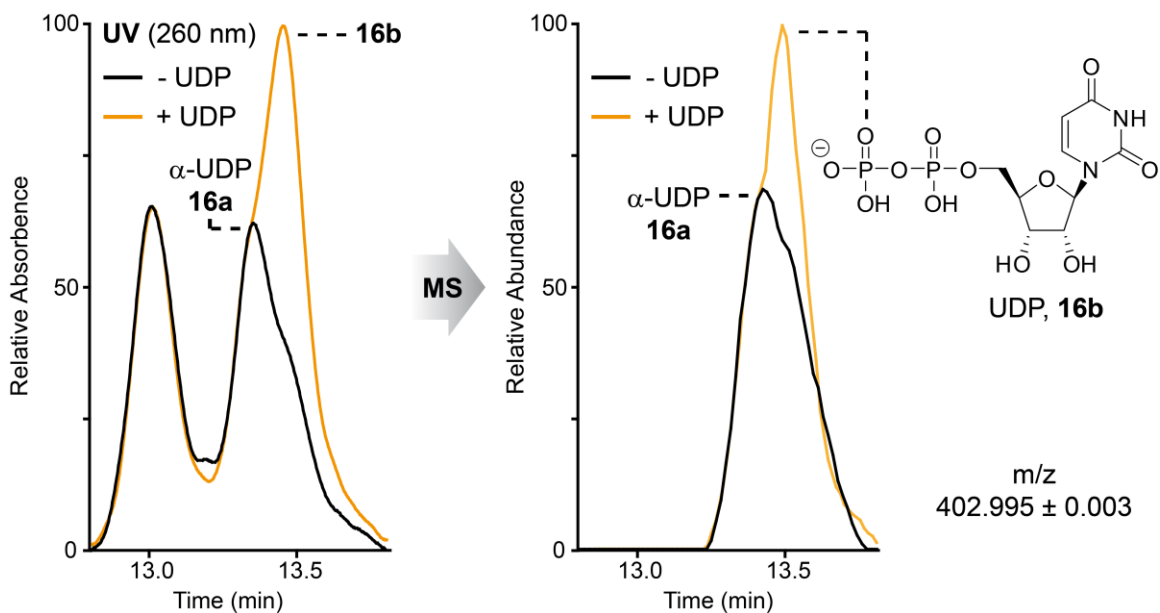
Fig. S9.

Co-injection study for β-5'-uridine-di-phosphate **16b**. For this experiment we used the same buffers as stated in the general information, but a different gradient: 0 → 15 min, Buffer B 0% → 10%. Co-injection was followed by UV and MS detection with commercially available material.
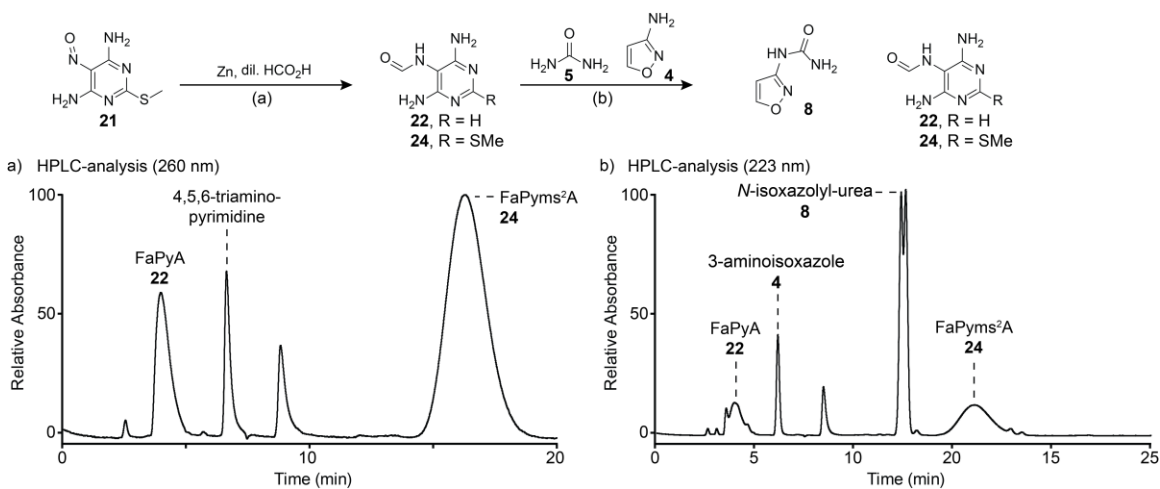
Fig. S10

Prebiotically linked syntheses of pyrimidine (**8**) and purine (**22**, **24**) precursors (detailed information can be found in the aforementioned procedure). a) prebiotically formed nitrosopyrimidine **21** was converted to **22** and **24** in the presence of Zn and dil. formic acid. The HPL-chromatogram of the reaction products is shown. b) The reaction from a) was directly used and a solution containing **4** and **5** was added. Upon dry-down the formation of **8** was observed in the presence of **22** and **24**. The HPL-chromatogram of the resulting products is shown.
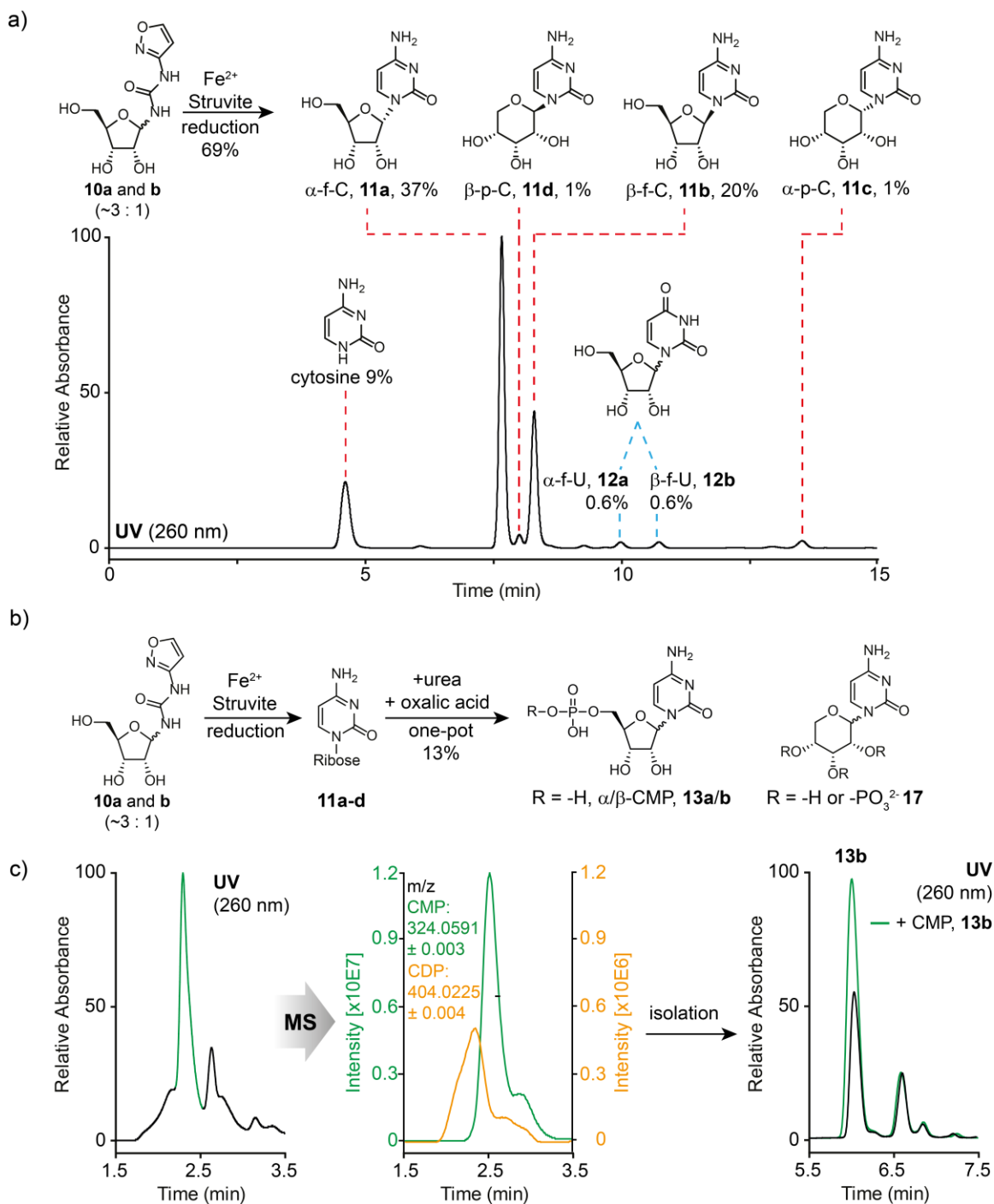
Fig. S11.

Formation of pyrimidine nucleotides from isoxazolylurea-ribosides with struvite. a) LC-MS analysis of pyrimidine nucleoside formation from compound **10a/b** in the presence of struvite. The UV-chromatogram at 260 nm is shown. The reduction of the isoxazole moiety in **10a/b** furnished the α and β-anomers as pyranoside (p) and furanside (f) isomers of cytidine (C, **11a-d**) or uridine (U, **12a/b**). b) One-pot Synthesis of cytidine mono- and di-phosphates (**13a/b-14a/b**) with struvite after urea and oxalic acid was

added to the reaction mixture shown in (a) and letting the mixture dry-down at 85°C for 20 h. c) LC-MS analysis of the corresponding nucleotide peaks and isolation from the prebiotic reaction. Co-injection studies confirmed formation of CMP (**13a/b**). The α- and β-anomers of CMP were not separable and therefore the UV peaks represent a mixture of both anomers.
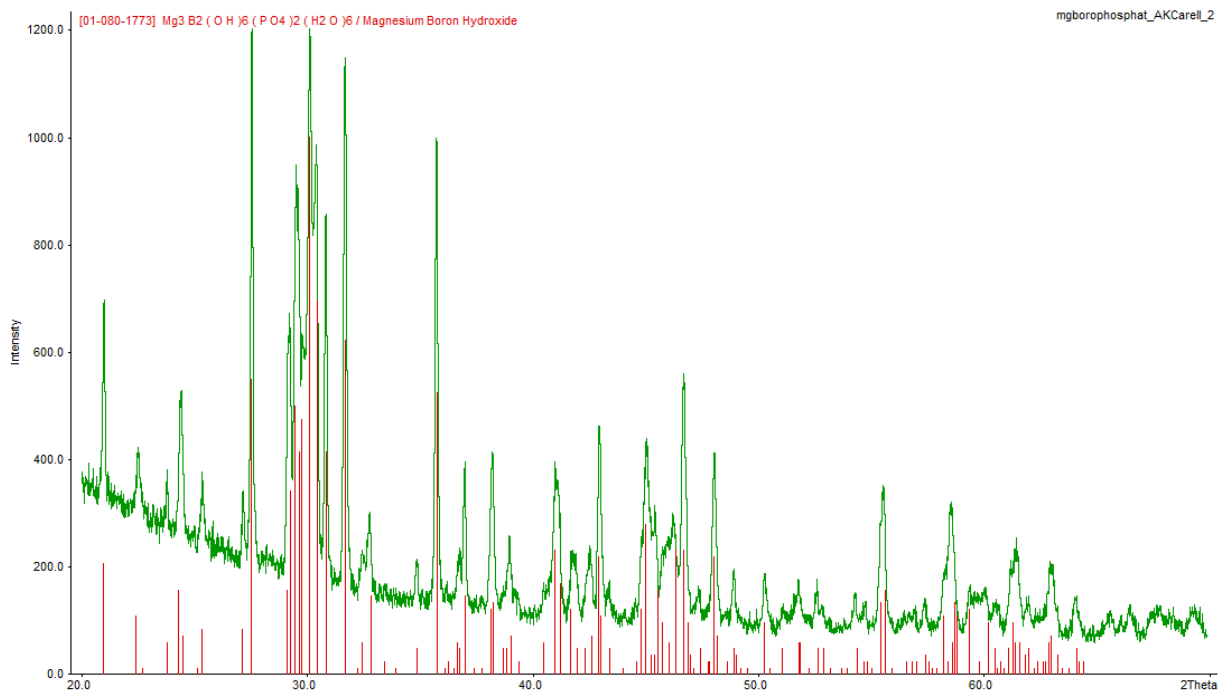
Fig. S12.

XRD measurement of synthetic lueneburgite (green) and comparison with database values (red).
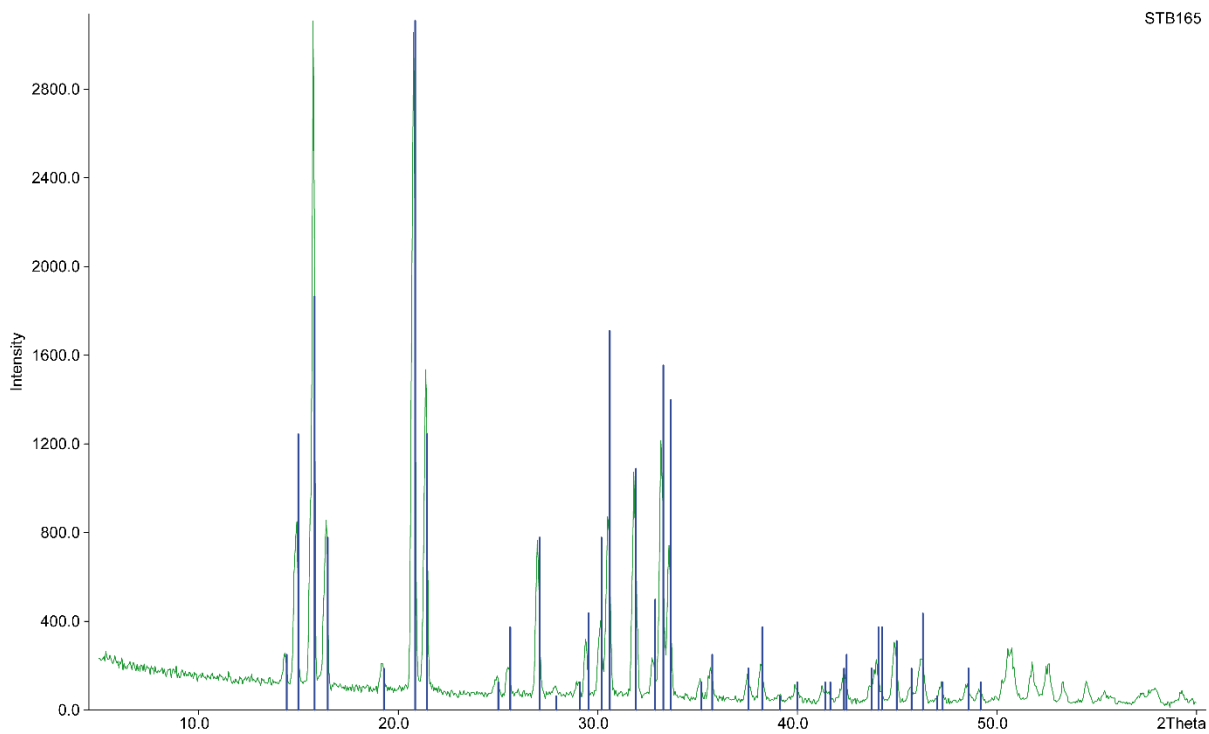
Fig. S13.

XRD measurement of synthetic struvite (green) and comparison with database values (blue).

References

1. J. A. Doudna, T. R. Cech, The chemical repertoire of natural ribozymes. *Nature* **418**, 222-228 (2002).
2. D. P. Horning, G. F. Joyce, Amplification of RNA by an RNA polymerase ribozyme. *Proc. Natl. Acad. Sci.* **113**, 9786-9791 (2016).
3. J. Attwater, A. Raguram, A. S. Morgunov, E. Gianni, P. Holliger, Ribozyme-catalysed RNA synthesis using triplet building blocks. *eLife* **7**, e35255 (2018).
4. W. Gilbert, Origin of life: The RNA world. *Nature* **319**, 618 (1986).
5. M. W. Powner, B. Gerland, J. D. Sutherland, Synthesis of activated pyrimidine ribonucleotides in prebiotically plausible conditions. *Nature* **459**, 239 (2009).
6. S. Becker *et al.*, A high-yielding, strictly regioselective prebiotic purine nucleoside formation pathway. *Science* **352**, 833-836 (2016).
7. H.-J. Kim, S. A. Benner, Prebiotic stereoselective synthesis of purine and noncanonical pyrimidine nucleotide from nucleobases and phosphorylated carbohydrates. *Proc. Natl. Acad. Sci.* **114**, 11315-11320 (2017).
8. S. Stairs *et al.*, Divergent prebiotic synthesis of pyrimidine and 8-oxo-purine ribonucleotides. *Nat. Commun.* **8**, 15270 (2017).
9. R. Saladino *et al.*, Meteorite-catalyzed syntheses of nucleosides and of other prebiotic compounds from formamide under proton irradiation. *Proc. Natl. Acad. Sci.* **112**, E2746-E2755 (2015).
10. J. Kasting, Earth's early atmosphere. *Science* **259**, 920-926 (1993).
11. P. B. Rimmer, O. Shorttle, Origin of Life's Building Blocks in Carbon- and Nitrogen-Rich Surface Hydrothermal Vents. *Life* **9**, 12 (2019).
12. W. Martin, J. Baross, D. Kelley, M. J. Russell, Hydrothermal vents and the origin of life. *Nat. Rev.s Microbiol.* **6**, 805 (2008).
13. E. Camprubi, S. F. Jordan, R. Vasiliadou, N. Lane, Iron catalysis at the origin of life. *IUBMB Life* **69**, 373-381 (2017).
14. S. A. Benner, H.-J. Kim, E. Biondi, in *Prebiotic Chemistry and Chemical Evolution of Nucleic Acids,* C. Menor-Salván, Ed. (Springer International Publishing, Cham, 2018), pp. 31-83.
15. S. Ranjan, Z. R. Todd, P. B. Rimmer, D. D. Sasselov, A. R. Babbin, Nitrogen Oxide Concentrations in Natural Waters on Early Earth. *Geochem. Geophys. Geosyst.* **20**, 2021-2039 (2019).
16. S. Becker *et al.*, Wet-dry cycles enable the parallel origin of canonical and non-canonical nucleosides by continuous synthesis. *Nat. Commun.* **9**, 163 (2018).
17. P. Thaddeus, The prebiotic molecules observed in the interstellar gas. *Philos. Trans. Royal Soc. B* **361**, 1681-1687 (2006).
18. R. A. Sanchez, J. P. Ferris, L. E. Orgel, Cyanoacetylene in Prebiotic Synthesis. *Science* **154**, 784-785 (1966).
19. B. H. Patel, C. Percivalle, D. J. Ritson, C. D. Duffy, J. D. Sutherland, Common origins of RNA, protein and lipid precursors in a cyanosulfidic protometabolism. *Nat. Chem.* **7**, 301 (2015).
20. H. Kofod, On the Isomerism of Hydroxyurea. I. Kinetics of the Reaction between Hydroxylammonium Ion and Cyanate Ion. *Acta Chem. Scand.* **7**, 274-279 (1953).
21. K. B. Muchowska, S. J. Varma, J. Moran, Synthesis and breakdown of universal metabolic precursors promoted by iron. *Nature* **569**, 104-107 (2019).

22. V. S. Airapetian, A. Glocer, G. Gronoff, E. Hébrard, W. Danchi, Prebiotic chemistry and atmospheric warming of early Earth by an active young Sun. *Nat. Geosci.* **9**, 452 (2016).

23. H. J. Cleaves, J. H. Chalmers, A. Lazcano, S. L. Miller, J. L. Bada, A Reassessment of Prebiotic Organic Synthesis in Neutral Planetary Atmospheres. *Orig. Life Evol. Biospheres* **38**, 105-115 (2008).

24. D. P. Summers, S. Chang, Prebiotic ammonia from reduction of nitrite by iron (II) on the early Earth. *Nature* **365**, 630-633 (1993).

25. R. Sukrit, T. Z. R., S. J. D., S. D. D., Sulfidic Anion Concentrations on Early Earth for Surficial Origins-of-Life Chemistry. *Astrobiology* **18**, 1023-1040 (2018).

26. G. K. Rollefson, C. F. Oldershaw, The reduction of nitrites to hydroxylamine by sulfites. *J. Am. Chem. Soc.* **54**, 977-979 (1932).

27. R. M. Hazen, Paleomineralogy of the Hadean Eon: A preliminary species list. *Am. J. Sci.* **313**, 807-843 (2013).

28. E. D. Swanner *et al.*, Cobalt and marine redox evolution. *Earth. Planet. Sci. Lett.* **390**, 253-263 (2014).

29. G. F. Joyce, The antiquity of RNA-based evolution. *Nature* **418**, 214 (2002).

30. D. M. Fialho *et al.*, Glycosylation of a model proto-RNA nucleobase with non-ribose sugars: implications for the prebiotic synthesis of nucleosides. *Org. Biomol. Chem.* **16**, 1263-1271 (2018).

31. K. Hyo-Joong *et al.*, Evaporite Borate-Containing Mineral Ensembles Make Phosphate Available and Regiospecifically Phosphorylate Ribonucleosides: Borate as a Multifaceted Problem Solver in Prebiotic Chemistry. *Angew. Chem. Int. Ed.* **55**, 15816-15820 (2016).

32. A. Ricardo, M. A. Carrigan, A. N. Olcott, S. A. Benner, Borate Minerals Stabilize Ribose. *Science* **303**, 196-196 (2004).

33. M. Kijima, Y. Nambu, T. Endo, Reduction of cyclic compounds having nitrogen-oxygen linkage by dihydrolipoamide-iron(II). *J. Org. Chem.* **50**, 1140-1142 (1985).

34. G. Wächtershäuser, Before enzymes and templates: theory of surface metabolism. *Microbiol. Rev.* **52**, 452-484 (1988).

35. U. Trinks, A. dir. Eschenmoser, ETH Zurich, Zurich (1987) (ETH e-collection 10.3929/ethz-a-000413538).

36. R. Krishnamurthy, On the Emergence of RNA. *Isr. J. Chem.* **55**, 837-850 (2015).

37. J. Liebig, F. Wöhler, Untersuchungen über die Cyansäure. *Ann. Phys.* **96**, 369-400 (1830).

38. M. Preiner *et al.*, A hydrogen dependent geochemical analogue of primordial carbon and energy metabolism. *bioRxiv*, 682955 (2019).

39. C. Bonfio *et al.*, Prebiotic iron–sulfur peptide catalysts generate a pH gradient across model membranes of late protocells. *Nat. Catal.* **1**, 616-623 (2018).

40. O. Trapp, J. Teichert, F. Kruse, Direct Prebiotic Pathway to DNA Nucleosides. *Angew. Chem. Int. Ed.* **0**.

41. J. Kofoed, J.-L. Reymond, T. Darbre, Prebiotic carbohydrate synthesis: zinc–proline catalyzes direct aqueous aldol reactions of α-hydroxy aldehydes and ketones. *Org. Biomol. Chem.* **3**, 1850-1855 (2005).

42. C. Meinert *et al.*, Ribose and related sugars from ultraviolet irradiation of interstellar ice analogs. *Science* **352**, 208-212 (2016).

43. K. Usami, A. Okamoto, Hydroxyapatite: catalyst for a one-pot pentose formation. *Org. Biomol. Chem.* **15**, 8888-8893 (2017).

44. S. Becker *et al.*, A high-yielding, strictly regioselective prebiotic purine nucleoside formation pathway. *Science* **352**, 833-836 (2016).

45. G. K. Rollefson, C. F. Oldershaw, The reduction of nitrites to hydroxylamine by sulfites. *J. Am. Chem. Soc.* **54**, 977-979 (1932).

46. S. Naiditch, D. M. Yost, The Rate and Mechanism of the Hydrolysis of Hydroxylamine Disulfonate Ion. *J. Am. Chem. Soc.* **63**, 2123-2127 (1941).

47. D. H. Shannahoff, R. A. Sanchez, 2,2'-Anhydropyrimidine nucleosides. Novel syntheses and reactions. *J. Org. Chem.* **38**, 593-598 (1973).

48. R. M. Davidson, E. White, S. A. Margolis, B. Coxon, Synthesis of nitrogen-15-labeled 2-amino(glycofurano)oxazolines via glycosylamine intermediates. *Carbohydr. Res.* **116**, 239-254 (1983).

49. R. U. Lemieux, T. L. Nagabhushan, B. Paul, Relationship of 13C to Vicinal 1H Coupling to the Torsion Angle in Uridine and Related Structures. *Can. J. Chem.* **50**, 773-776 (1972).

50. W. Berdesinski, Synthetische Darstellung von Lüneburgit. *Naturwissenschaften* **38**, 476-477 (1951).

51. V. V. Vol'khin *et al.*, Synthesis of struvite ($MgNH_4PO_4 \cdot 6H_2O$) and its use for sorption of nickel ions. *Russ. J. Appl. Chem.* **88**, 1986-1996 (2015).